University of Tartu
Faculty of Social Sciences
School of Economics and Business Administration

Ariana Paola Cortés Ángel

Deep Diving into the S&P 350 Europe Index Network and Its Reaction to the COVID-19

MASTER'S THESIS

Supervisor: M. Hakan Eratalay

Tartu, 2021

I have written this Thesis independently. Any ideas or data taken from other authors or other sources have been fully referenced.

Abstract

We calculate global and local parameters with the partial correlation network of the S&P 350 Europe index as a base. To the best of my knowledge, this is the first time in the financial networks literature that the radius is calculated, complementing with it, the diameter and average distance parameters. These three last parameters allow us to deduce the force that an economic instability should exert to trigger a cascade effect on the network. Local parameters help us gauge the importance of the companies regarding different aspects, like the strength of the relationships with their neighborhood and their location in the network. By introducing the skeleton concept of a dynamic network, we detected the stability of relations among constituents, and we noticed an important increase in these stable connections during the COVID-19 pandemic. In addition, for the first time in financial networks literature, a homophilic profile was carried out, and we found highly homophilic relationships among companies, considering firms by country and industry.

Keywords: Financial Networks, Centralities, Homophily, Multivariate, Networks Connectivity

JEL Clasification: C32, C58, G15.

Contents

List of Figures **iv**

List of Tables **vi**

1 Introduction **1**

2 Literature Review **5**
2.1 Network Analysis 6
2.2 Financial Networks 7

3 Data **9**

4 Methodology **13**
4.1 Econometrical Analysis 13
4.2 Network Analysis 17
4.3 Centralities 22
4.4 Homophily 25
4.5 Network Skeleton 27

5 Results and Analysis **29**
5.1 Global Measures 30
5.2 Local Measures 33
5.3 Homophily 36
5.4 Skeleton 39

6 Conclusions **47**

A Appendix **50**
A.1 Radius versus Average Path Length 50
A.2 Tables and Figures 50

Bibliography **92**

Symbol Index **93**

List of Figures

3.1 S&P Europe 350 Index Prices 10
3.2 S&P Europe 350 Index Prices 11
3.3 S&P Europe 350 Index Returns 12
3.4 Descriptive Statistics for S&P Europe 350 Index Returns . . . 12

4.1 A weighted graph G and its adjacency matrix $\mathbf{A}$. 19
4.2 Homophilic and Heterophilic Networks 27
4.3 Network Skeleton 28

5.1 Weights of Positive and Negative Edges 31
5.2 Partial Correlation Distribution 32

A.1 Radius and Average Path Length 50
A.2 Net, Absolute, and Positive Weights Over Time 51
A.3 Positive Global Measures Over Time 52
A.4 Absolute Global Measures Over Time 53
A.5 Net Partial Correlation Networks by Country 72
A.6 Net Partial Correlation Networks by Sector 73
A.7 Positive Partial Correlation Networks by Country 74
A.8 Positive Partial Correlation Networks by Sector 75
A.9 Net Skeleton Homophily by Country 76
A.10 Net Skeleton Homophily by Sector 77

List of Tables

5.1 Positive and Negative Edges 31
5.2 Global measures 33
5.3 Top 1 centralities 34
5.4 Simultaneous effects Top 20, positive and absolute values . . . 36
5.5 Homophily by Country 37
5.6 Homophily by Industry 38
5.7 Daily Networks: Edge Statistics by Periods 39
5.8 Period Skeletons: Global Measures 40
5.9 84-Day Skeletons: Global Measures 41
5.10 Period Skeletons: Degree Centrality 42
5.11 Period Skeletons: Eigenvector Centrality 43
5.12 Period Skeletons: Closeness Centrality 44
5.13 Period Skeletons: Harmonic Centrality 44
5.14 Period Skeletons: Betweenness Centrality 45
5.15 Homophily Over the Skeletons 46

A.1 Average Net Degree Centrality Top 20 54
A.2 Average Absolute Degree Centrality Top 20 55
A.3 Average Positive Degree Centrality Top 20 56
A.4 Average Absolute Closeness Centrality Top 20 57
A.5 Average Positive Closeness Centrality Top 20 58
A.6 Average Absolute Harmonic Centrality Top 20 59
A.7 Average Positive Harmonic Centrality Top 20 60
A.8 Average Absolute Eigenvector Centrality Top 20 61
A.9 Average Positive Eigenvector Centrality Top 20 62
A.10 Average Absolute Betweenness Centrality Top 20 63
A.11 Average Positive Betweenness Centrality Top 20 64
A.12 Average Centralities by Sector Part I 65
A.13 Average Centralities by Sector Part I 66

A.14 Average Centralities by Sector Part III 67
A.15 Average Centralities by Sector Part IV 68
A.16 Average Centralities by Country 69
A.17 Network Description by Country 70
A.18 Table Title 71
A.19 Firms Part I 78
A.20 Firms Part II 79
A.21 Firms Part III 80
A.22 Firms Part IV 81
A.23 Firms Part V 82
A.24 Firms Part VI 83
A.25 Firms Part VII 84
A.26 Firms Part VIII 85
A.27 Firms Part IX 86
A.28 Firms Part X 87
A.29 Countries 87
A.30 Industries 88

1 Introduction

The global financial crisis that occurred in 2007-2008 has encouraged researchers to apply an interdisciplinary approach to studying the systemic risk in the financial sector to predict and control it. However, before this can occur, it is necessary to understand and model it. Caccioli, Barucca, and Kobayashi 2018 delve into this topic, utilizing network analysis as their primary tool.

From this moment, we can say that the interest in understanding the topology of financial networks was born to realize its possible reaction when being impacted by economic instability and the possible consequences that this shock entails.

This thesis aims to analyze the network's topology derived from the interrelationships between the shares of the European stock market, particularly the S&P Europe index, considering adjusted closing prices from January 2016 to September 2020. We especially want to know which firms are the most central in the dynamic network, how the connectedness of the graph evolves under the influence of the pandemic shock, and determine if the network links follow a homophilic behavior.

In general, the network analysis on financial networks has primarily focused on the study of over a handful of graph parameters, like diameter, average path length, and centralities (Anufriev and Panchenko 2015, Diebold and Yılmaz 2014, and Kuzubaş, Ömercikoğlu, and Saltoğlu 2014 to mention some). Two of the main topics studied over a network are its connectivity and centrality. Each of these terms tends to be used for several distinct concepts depending on the taste and needs of the authors. For this reason, the centrality has been divided into different types, which allows avoiding confusion while simultaneously studying different vertices characteristics. In contrast, connectivity often could mean the number of links of the network, the strength of the links between nodes, the average number of neighbors for a vertex, or the number of disjoints paths between a pair of nodes, among other interpretations. In this thesis, we will use two connectivities: the network connectivity, i.e., its number of edges, and local connectivity of a node, meaning its number of adjacent neighbors.

We use the consistent dynamic conditional correlation model (cDCC-GARCH), the multivariate model presented by Aielli 2013. Following the same theoretical approach as in Eratalay and Vladimirov 2020, we obtain the partial correlation network by applying the Gaussian graphic model algorithm (GGM). This GGM model is used instead of computing the inverse of the conditional correlation matrix since the complexity of this computation could be expensive according to its dimension, in our case 331×331-matrix, facilitating its calculation. The GGM is used to obtain partial correlations in biochemestry (Krumsiek et al. 2011), psychology (Epskamp et al. 2018) to mention some, in addition to financial networks like Anufriev and Panchenko 2015.

Then we obtain global and local measurements of the network to identify which companies are most sensitive to external changes given the structure of the system; for this, we will rely on Demirer et al. 2018, and Kuzubaş, Ömercikoğlu, and Saltoğlu 2014 for two additional measures of centrality:

betweenness and closeness.

We calculate the radius of the partial correlation network, a parameter of global centrality that has not been calculated for financial networks to the best of my knowledge. Assuming that a shock has a single node as an entry point from which it will spread throughout the network, the diameter and radius can be interpreted as the minimum force a shock should have to ensure its propagation all over the network in two different scenarios: the diameter, when the entry point is unknown, and the radius, when the entry point can be selected. On the other hand, the average path length shows the average force needed for the shock transmission between any pair of vertices. With this contribution, we found a sharper bound for the force of an economic instability needed to trigger a cascade effect on the network.

We perform a homophilic profile, where we measure the tendency of the edges of the network to create bonds with similar nodes; we found a direct relationship between the partial correlations and the proportion of homophilic edges, which helps us get a clearer perspective into the underlying network structure. Homophily is a novel approach since, regardless of being a well-known topic in social sciences, it has been barely mentioned in the financial networks literature, such as Elliott, Hazell, and Georg 2020, and Barigozzi and Brownlees 2019 where it is referred to as similarity. Moreover, based on the daily network pictures, we capture the system's dynamics by introducing the concept of the skeleton of a dynamic network, which may be used as a forecast enhancing tool or interpreted as a shock strength measure.

Thanks to the analysis of a new substructure, we found out that during the Covid-19 pandemic there was an increase in the number of stable relationships.

What remains of this work is structured as follows. In Chapter 2, we make a literature review of Network Analysis and Financial Networks. In Chapter 3, we describe the data under study. Later, in Chapter 4, we present the methodology implemented for Financial Econometrics and Network Analysis. In Chapter 5, we analyze the results, and in Chapter 6, we conclude.

2 Literature Review

This thesis focuses on the methodology to obtain and analyze some of the most representative global and local centrality measures of a network, allowing us to map the topology of the network under study. The idea is that these measures serve as input in systemic risk studies, being able to be complemented with more information as well as the risk profile of each firm and its balance sheet, among others.

We concentrate on the radius, diameter, and average distance and the degree, closeness, and betweenness centralities, additionally developing a homophilic profile. Introducing the calculation of the radius in the financial networks; and the definition of the skeleton of a dynamic network, which results from collecting the resilient edges over time.

By analyzing centralities, central banks can identify Global Systemically Important Institutions (G-SIIs), which can help regulate them, as already suggested in several other studies. For instance, the work of Martinez-Jaramillo et al. 2014 bases a large part of its analysis on the topology of the interbank network, creating a measure of centrality composed of the closeness, betweenness, and the degree centralities (being the latter called strength). Kuzubaş, Ömercikoğlu, and Saltoğlu 2014 take as an example the Turkish crisis that occurred in 2000, and in addition to the degree, closeness, and betweenness centralities, they calculate the Bonacich centrality. These two studies describe the interbank network.

Several more articles develop the centralities, focusing mainly on the degree and eigenvector such as Millington and Niranjan 2020 and Anufriev and Panchenko 2015, or Iori and Mantegna 2018 where the average distance is added to their analysis, and Billio et al. 2012 who calculate the proximity and eigenvector.

2.1 Network Analysis

During the 1960s and 1970s, several mathematical and statistical tools started to be used by social scientists to get a better understanding of the structure and behavior of social networks (Milgram 1967, Zachary 1977, Killworth and Bernard 1978). While the statistical tools are used to obtain quantitative results, the mathematical devices borrowed from graph theory allow us to discover and visualize the underlying structure of the studied data.

In the late 20th century and the beginning of the 21st century, with the seminal works made by Albert, Jeong, and Barabási 1999, Faloutsos, Faloutsos, and Faloutsos 1999, and Watts and Strogatz 1998, among others, the above mention set of tools, combined with the growing availability of information to the general public and the increased computational power to analyze big data sets led to the creation of network theory as a discipline on its own. Since then, this type of research was applied to study a wide variety of topics, such as genomics, epidemics, cybersecurity, communication, financial markets, social interactions, linguistics and more (Lewis 2011, Keeling and Eames 2005, Solé et al. 2010).

The primary strength of network analysis lies in the fact that it incorporates a multidisciplinary approach that utilizes a range of theories, from social sciences such as economics to exact sciences such as biology. A great amount of detail about this can be found in Jackson 2011, who suggests that all that is needed for this approach is to identify agents and relationships that connect them. For instance, using the labor market to understand searching and matching models, or using social networks to analyze human behavior.

2.2 Financial Networks

The financial network is one example of a complex system, where there are many actors (financial institutions, mainly interbank connections have been studied) and an uncountable number of interrelations among them. Caccioli, Barucca, and Kobayashi 2018 delve into systemic risk, utilizing network analysis as their primary tool.

The application of network theory to financial networks has shown that high connectivity can produce one of two effects when a disruption to the system occurs, absorption (Allen and Gale 2000, Freixas, Parigi, and Rochet 2000) or contagion (Gai and Kapadia 2010, Elliott, Golub, and Jackson 2014). If the disruption to the system is minor and within a certain threshold, the connectivity of the network helps to alleviate the shock, which can be interpreted as absorption. However, if the disruption exceeds the threshold, instead of softening the impact, the interconnections augment the spread of it, as shown in Acemoglu, Ozdaglar, and Tahbaz-Salehi 2015.

The relationships in a network can be direct or indirect. One example of a direct network is the interbank market, where the relationship is the trade of currency executed directly by the banks Allen and Babus 2009.

In our case, the relationship is indirect and describes how the behavior of one company can lead to the behavior of others in response; as an example, we can imagine that there is a waltz, where the couples are the firms, there are several couples, they may or may not know each other, but they all dance considering the movements of the other couples.

We derive this relationship from the partial correlation matrix. This method has been widely applied and modified, to mention some Kenett et al. 2010, Anufriev and Panchenko 2015 and Iori and Mantegna 2018 write a compendium of several studies and their different applications, some of them using this same approach, all with the idea of understanding how a network reacts to disruption more in-depth.

Many studies of financial systemic risk based on network theory have been developed since 2007, that consider a worldwide assortment of components, such as in Diebold and Yilmaz 2009, which assesses equity stocks of developed and emerging countries, or Anufriev and Panchenko 2015, considering the Australian market or Diebold and Yilmaz 2015 among U.S. and Europe contexts.

3 Data

We use the S&P Europe 350 index, which is made up of 350 blue-chip companies from 16 different developed European countries. This index is a weighted, float-adjusted market capitalization, that is, it only considers the shares available to investors in public markets. This index provides us with a significant sample of the European stock market, which is why we take it as the basis for this study, which mainly focuses on the methodology of the study of financial networks.

The S&P Europe 350 index components, along with their market capitalizations and tickers, were directly provided by Standard and Poors, with figures of December 2019; with this list, we gather their daily adjusted closure history from January 2014 to October 2020 from Yahoo Finance. Data for the Morgan and Stanley World Index (MSWI) was also collected, same dates and source.

From the raw data received, we only consider synchronized periods of information, since not all the firms had data in the same periods the number of observations were reduced, both for the 350 Europe index and for the MSWI. We also found companies that belonged to the same group or association so their repeated data was removed for these companies, otherwise results would be contaminated, showing an evident correlation.

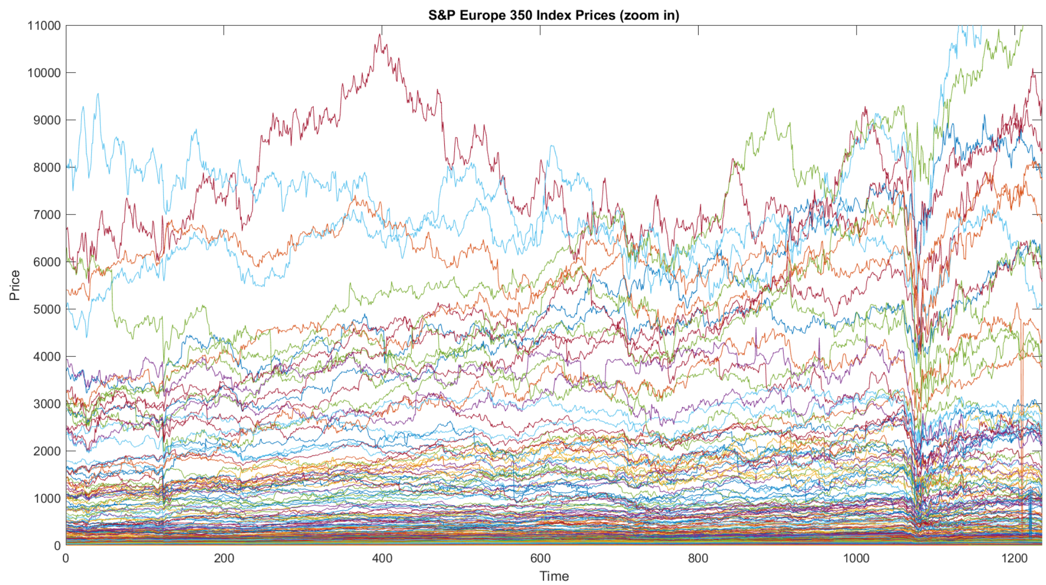

Figure 3.1: S&P Europe 350 index prices from January 2016 to September 2020 without considering Lindt & Sprungli AG Reg since its prices are too much greater than the rest, just for better visualization. Source: author's calculation.

The S&P 350 Europe index was left with 331 firms after this initial treatment, considering now from January 2016 to September 2020, the same period was taken into account for the MSWI index. These trading dates correspond only to business days, so there are no weekends nor holidays, with approximately 250 business days in a year, and a total of 1,202 days for the whole period.

For all firms, we calculated their log-returns and after that we treated the data with a generalized Hampel filter, using a 20 days moving data window, on average 0.42% of the data was an outlier, details about this method can be found in Pearson et al. 2015.

The COVID pandemic started to become evident in Europe by the end of February 2020, Plümper and Neumayer 2020, we can observe in Figure 3.3 a significant increase in the index volatility, and a sudden fall in prices in Figure 3.2 by the beginning of March 2020, being a consistent reaction to the pandemic shock.

Given that our data consist of 331 firms with 1,201 observations each, we use box plots to sum up all their descriptive statistics; since the attributes of this graphic tool make easier to understand the behavior of large amount of data. From the descriptive statistics in the box plot Figure 3.4, we can notice that the returns lie around zero; with a standard deviation of around two; in average, returns are slightly negatively skewed, but there are several values less than minus one, implying that its distribution is highly negatively skewed; their kurtosis is in average nine, suggesting a leptokurtic distribution.

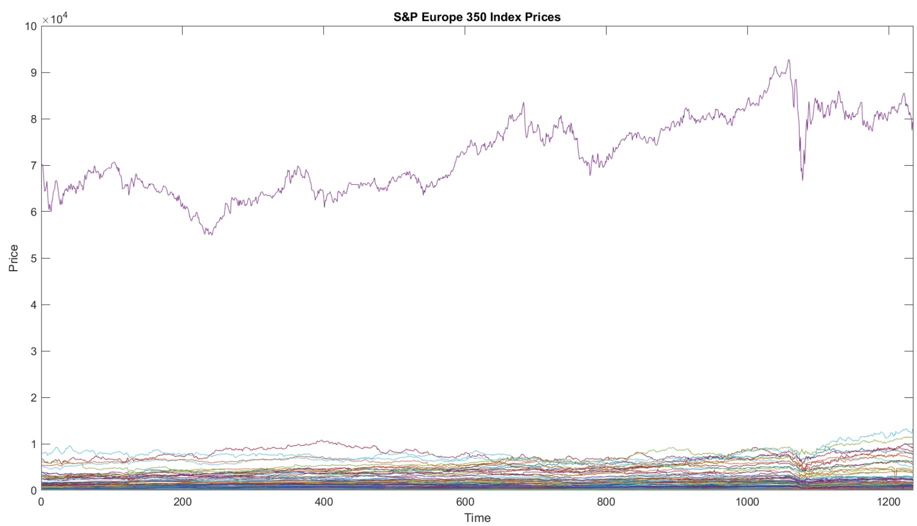

Figure 3.2: S&P Europe 350 index prices from January 2016 to September 2020. *Source:* Author's calculations.

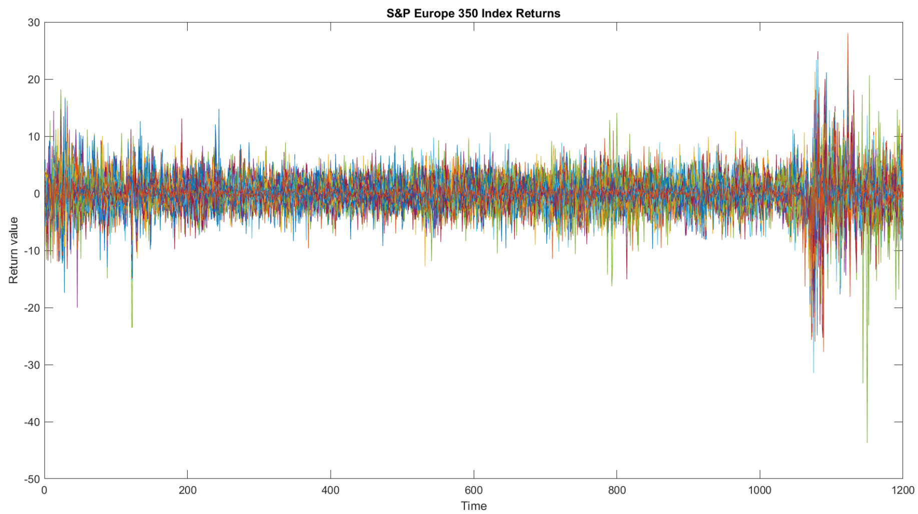

Figure 3.3: S&P Europe 350 Index Returns from January 2016 to September 2020. By the beginning of March 2020, we can notice a sudden increase in the volatility. *Source:* Author's calculations.

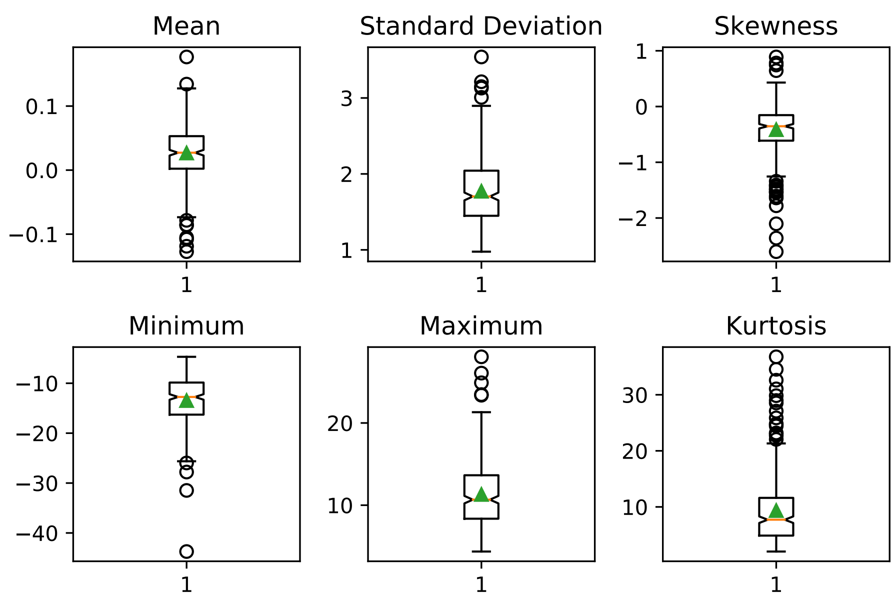

Figure 3.4: Descriptive statistics of the S&P Europe 350 index returns from January 2016 to September 2020. *Source:* Author's calculations.

4 Methodology

The methodology will be divided in two main parts, the econometrical approach and the network approach.

4.1 Econometrical Analysis

The econometric analysis will be based mainly on Eratalay and Vladimirov 2020 work, but in this case, it will not consider an unobservable factor since estimating its parameters is expensive given the number of components; instead, we will consider the Morgan Stanley World Index (MSCI) as a common observable factor; we include this common factor to avoid increasing network connectivity by diminishing data bias. We chose MSCI as it is a guide to the behavior of developed economies worldwide; more detail about common factors can be found in Barigozzi and Brownlees 2019.

This analysis will be done in three main steps. First, we will measure the conditional mean, then the conditional variance, and finally, we will calculate the time-varying conditional correlations, with the multivariate model presented by Aielli 2013.

A return can be represented by the conditional mean and the conditional variance:

$$r_t = \mathbb{E}_t(r_t \mid I_{t-1}) + \sqrt{\mathbb{V}ar_t(r_t \mid I_{t-1})}\varepsilon_t \tag{4.1}$$

With ε_t representing the standardized disturbance, $\varepsilon_t \sim N(0, 1)$. The conditional mean and the conditional variance depend on the previous information.

Conditional Expectation

For estimating the conditional expectation, $\mathbb{E}_t(r_t \mid I_{t-1})$, we will use a vector autoregressive model, VAR(1).

$$r_t = \mu + \delta r_{t-1} + \zeta r_{t-1}^M + \eta_t \tag{4.2}$$

Where μ is a $n \times 1$ column vector representing the intercept; δ and ζ, are $n \times n$ matrices of parameters of the returns lagged one period, from S&P Europe 350 and Morgan Stanley world indices respectively, in particular ζ is a diagonal matrix; and η_t is the error term represented by a random process with mean zero and variance h_t, $\eta_t = \sqrt{h_t}\varepsilon_t$, and ε_t are the standardized errors.

Conditional Variance

Let us denote the conditional variance and the conditional mean, h_t and μ_t, respectively, therefore the error term can be expressed η_t as:

$$\eta_t = r_t - \mu_t = \sqrt{h_t}\varepsilon_t, \text{ where } \eta_t \sim N(0, h_t) \tag{4.3}$$

For each time series the conditional variance of the error term can be represented as a GARCH(1,1):

$$\begin{aligned} h_{t+1,i} &= \omega_i + \alpha_i (r_{t,i} - \mu_{t,i})^2 + \beta h_{t,i} \\ &= \omega_i + \alpha_i h_{t,i} \varepsilon_{t,i}^2 + \beta_i h_{t,i} \\ &= \omega_i + \alpha_i \eta_i^2 + \beta_i h_{t,i} \end{aligned} \tag{4.4}$$

where the parameters $\omega > 0$, $\alpha \geq 0$, $\beta \geq 0$ and $\alpha + \beta < 1$, hence each h_t is stationary.

Summing up, we represent all the conditional covariances and variances in the covariance-variance matrix, $\mathbf{H}_t$, expressed below:

$$\mathbf{H}_t = \mathbf{D}_t \mathbf{R}_t \mathbf{D}_t \tag{4.5}$$

$$\mathbf{D}_t = \operatorname{diag}\{\sqrt{h_{t,i}}\} \tag{4.6}$$

Where $\mathbf{H}_t$ depends on $\mathbf{R}_t$, the correlation matrix, and $\mathbf{D}_t$, a diagonal matrix of the standard deviation of the conditional variance.

Time-Varying Conditional Correlations

The conditional returns $r_t = (r_{1t}, r_{2t}, \ldots, r_{nt})'$ and the standardized disturbances $\varepsilon_t = (\varepsilon_{1t}, \varepsilon_{2t}, \ldots, \varepsilon_{nt})'$ of n firms, where $r_t \mid I_{t-1} \sim N(\mu_t, \mathbf{H_t})$, and $\varepsilon_t \sim N(0, \mathbf{I}_n)$ respectively; with $\mathbf{H}_t = \mathbb{E}(r_t r_t' \mid I_{t-1})$ and $r_t = \mu_t + \mathbf{H_t}^{1/2} \varepsilon_t$.

Where $\mathbf{R}_t$ is the matrix of conditional correlations, therefore each of its elements is in the interval $[-1, 1]$ and, by (4.5), $\mathbf{R}_t$ should be positive definitive in order for $\mathbf{H}_t$ to be positive definite as well.

$$\mathbf{R}_t = \mathbf{Q}_t^{*-1} \mathbf{Q}_t \mathbf{Q}_t^{*-1} \tag{4.7}$$

$$\mathbf{Q}_t^{*-1} = \begin{bmatrix} 1/\sqrt{q_{11t}} & 0 & \dots & 0 \\ 0 & 1/\sqrt{q_{22t}} & \dots & 0 \\ \vdots & \vdots & \ddots & \vdots \\ 0 & 0 & \dots & 1/\sqrt{q_{nnt}} \end{bmatrix} \tag{4.8}$$

$$\mathbf{Q}_t = (1-\theta-\kappa)\bar{\mathbf{Q}} + \theta\{\mathbf{Q}_{t-1}^{*}\varepsilon_{t-1}\varepsilon_{t-1}'\mathbf{Q}_{t-1}^{*}\} + \kappa\mathbf{Q}_{t-1} \tag{4.9}$$

Where $\varepsilon_t^* = \mathbf{Q}_t^*\varepsilon_t$ and $\varepsilon_t^{*'} = \varepsilon_t'\mathbf{Q}_t^*$, using this notation we can simplify the previous equation.

$$\mathbf{Q}_t = (1-\theta-\kappa)\bar{\mathbf{Q}} + \theta\{\varepsilon_{t-1}^{*}\varepsilon_{t-1}^{*'}\} + \kappa\mathbf{Q}_{t-1} \tag{4.10}$$

$$\bar{\mathbf{Q}} = \mathbb{C}ov(\varepsilon_t^*\varepsilon_t^{*'}) = \mathbb{E}(\varepsilon_t^*\varepsilon_t^{*'}) \tag{4.11}$$

Where $\kappa \geq 0$ and $\theta \geq 0$ are scalars ensuring $\kappa + \theta < 1$, and $\bar{\mathbf{Q}}$ represents the unconditional covariance of the standardized distrubances, also known as long run covariance matrix, and for this work it will be replaced by the sample covariance of standardized residuals.

The estimation for the conditional mean, conditional variance and conditional correlation parameters is realized by the three step estimation following the Eratalay and Vladimirov 2020 path, this estimators are consistent and asymptotically normal in finite samples, more details in Carnero and Eratalay 2014.

4.2 Network Analysis

Once we have the conditional correlation matrix, we compute the partial correlation matrix using the GGM algorithm. From this partial correlation matrix, we construct our network, where a vertex will represent each firm, and the strength of the correlation between them will be represented by edges.

It should be noted that partial correlations range is $[-1, 1]$, and the partial correlation matrix will be a symmetric arrangement of entries within the same range, this matrix is the adjacency matrix of our network. We will consider an edge in all the cases except when $a_{ij} = 0$, which means that there is not a linear interdependence among i and j.

Formally, a *graph* or *network*, denoted by G, is an ordered pair of disjoint sets $(V(G), E(G))$, where $V(G)$ is a nonempty set of *vertices* or *nodes*, and $E(G)$ is the set of *edges* or *links*, where each edge is an unordered pair of distinct vertices $\{i, j\}$ simply denoted as ij[1]. Whenever two nodes i and j form a link ij, it is said that they are *adjacent* with each other, and that they are *neighbors*. Also, that the edge ij is incident to i and to j and viceversa. Moreover, i and j are called the *endvertices* (or *endnodes*, or simply *ends*) of ij, and is said that the edge *joins* i and j.

The simplest parameters of a network G are its number of vertices, called the *order* of G and denoted by N, and its number of edges, called the *size* of G and denoted by $m(G)$.

The most usual way to visually represent a graph is a diagram where each

[1] Although edges that go from one vertex to itself (called *loops*) can be defined, they have no useful interpretation within the scope of this study.

node is represented by a point or small circle and an edge is represented by a line that connects its end-vertices without crossing over any other vertex. Any graph of n vertices can be represented by a $n \times n$ matrix $\mathbf{A}$, called its *adjacency matrix*, where the entry a_{ij} of $\mathbf{A}$ is equal to 1 if there is an edge between the nodes i and j, or $a_{ij} = 0$ otherwise.

When modeling some practical problems, we could assign a real number $w(ij)$ to every link ij, called its *weight*[2]. In such case, a graph G together with the collection of weights on its edges is called a *weighted graph*, and we can add this extra information into the adjacency matrix of G, so instead of 0's and 1's we have that $a_{ij} = w(ij)$. This allows us to represent into the adjacency matrix, not only the existence of a relation between the endvertices of a link, but also take into account some characteristic that allows us to quantitatively differentiate between links, depending on the context.

In fact there is a one-to-one correspondence between symmetric matrices and weighted graphs, which allows us to define a network from any such matrix. In our case, the partial correlation matrices will play the role of the adjacency matrices of our graphs, where its values represent how close the co-movement of two firms are, i.e., how similar is their behaviour over time. This way, the weight $w(ij)$ of the link ij will be equal to the partial correlation between the two corresponding firms.

Given two graphs G and H, it is said that H is a *subgraph* (*subnetwork*) of G whenever $V(H) \subseteq V(G)$ and $E(H) \subseteq E(G)$, i.e., all the nodes and links of H are also contained in G. If G is weighted, then the *weight of the*

[2] For instance, such values could represent the cost of communicating or the distance between two locations, or the flow capacity in a tranportation network, or the strenght of the relationship between the elements, etc.

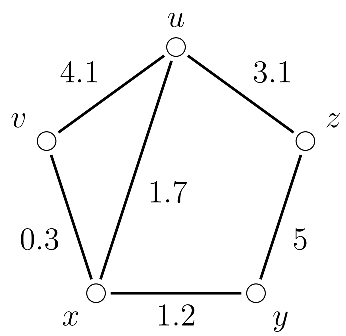

G

	u	v	x	y	z
u	0	4.1	1.7	0	3.1
v	4.1	0	0.3	0	0
x	1.7	0.3	0	1.2	0
y	0	0	1.2	0	5
z	3.1	0	0	5	0

$\mathbf{A}$

Figure 4.1: A weighted graph G and its adjacency matrix $\mathbf{A}$.

subgraph H is the sum of weights of all the links in H, in other words,

$$w(H) = \sum_{ij \in E(H)} w(ij). \tag{4.12}$$

Additionally, in any network, a *path* between vertices i and j is a sequence of distinct vertices $x_0, x_1, \ldots, x_k$, where $i = x_0$ and $j = x_k$, such that x_i and x_{i+1} form an edge in the network. For unweighted graphs the integer k represents the *length* of such path, i.e., the number of edges contained in the path; while for weighted networks the length of the path is the sum of the weight of its edges, i.e., is equal to the weight of the path. Any shortest path connecting i and j is called a *geodesic* and its length is called the *distance* between its endvertices, denoted by $d(i, j)$. In other words, the distance between two vertices is the minimum length that separates one node from the other. If there is no path connecting two nodes, the distance between them is defined as infinite.

Before continuing, we first need to highlight an important aspect of a distance metric. Distance is a value that represents how close related are two objects in the following way: the lower the value, the closer those objects are[3]. In contrast, the higher partial correlation between two firms is, the more related they are.

Therefore, it is necessary to reverse the order of the partial correlations so the respective new values can be handled like a proper distance metric (Opsahl, Agneessens, and Skvoretz 2010), where lower values correspond to closeness. For this reason, we will use the inverse of the weight for each link whenever we calculate lengths and distances, in other words, a new weight $w^*(ij) = [w(ij)]^{-1}$ is assigned to each edge when computing any distance related measure in the network.

From here, three relevant graph parameters are directly derived. First, the *average path length* of a graph G, denoted by $\overline{d}(G)$, is defined as the average distance between every pair of nodes in the network, i.e.,

$$\overline{d}(G) = \frac{1}{\binom{n}{2}} \sum_{i \neq j} d(i,j). \tag{4.13}$$

Second, the *radius* of G is the minimum length k such that there is a node whose distance to any other node is at most k, and is denoted by $\mathrm{rad}(G)$. And, finally the *diameter* of G, denoted by $\mathrm{diam}(G)$, is the maximum distance between any two nodes in the graph. Clearly, the following inequalities hold

$$\mathrm{rad}(G) \leq \mathrm{diam}(G) \qquad \text{and} \qquad \overline{d}(G) \leq \mathrm{diam}(G)^{[4]}. \tag{4.14}$$

[3] To get into the mathematical theory behind metric spaces go to Willard 2012.

These three parameters together tell us, respectively, the minimum, average, and maximum distance that we expect to cover from one random node to reach all the other nodes, in other words, they measure how strong a shock has to be in order to propagate over all the network despite its starting point.

It is worth mentioning that there are some graphs on which a proper distance can not be defined. When defining a distance on a network we are implicitly looking at an optimization problem where we want to find the shortest or cheapest way to move between any pair of nodes, and we are guaranteed to find a solution to this problem, and therefore define a distance, provided that all weights assigned to the edges are positive.

Unfortunately, when dealing with negative values, this task can not be fulfilled whenever there is a *negative cycle*, that is a sequence of distinct vertices $C = x_1, x_2, \ldots, x_k$ such that every pair of consecutive nodes form an edge and $x_1 x_k$ is also an edge, and $w(C) < 0$. In such case, the minimization problem has no solution since any path connected to this negative cycle can become cheaper and cheaper by walking inside the negative cycle and looping indefinitely. On the bright side, despite the fact that some algorithms (like Dijkstra's) are not designed to handle negative weights and fall into an infinite loop, there are some that can determine if there is any negative cycle, namely Bellman-Ford's algorithm.

---

[4] The radius and average path length cannot be related with an inequality since there are graphs whose radius is greater than, or less than, or equal to the average path length. See Figure A.1.

4.3 Centralities

Centrality measures are tools that allow us to quantify the importance or influence that a vertex has over the network as a whole or in a locally delimited region.

For unweighted graphs the *degree centrality* of a vertex i, denoted by $C_D(i)$, is the number of nieghbors that such node has, while for weighted graphs the degree centrality of i is the sum of the weights of all the edges incident to i[5]. However, since our focus is over networks where the weights of its links are in the interval $[-1, 1]$ we will distinguish between three degree centralities:

$$C_D^{net}(i) = \sum_j w^*(ij), \tag{4.15}$$

$$C_D^{abs}(i) = \sum_j |w^*(ij)|, \tag{4.16}$$

$$C_D^{+}(i) = \sum_{w^*(ij)>0} w^*(ij). \tag{4.17}$$

We will call these the *net degree centrality*, *absolute degree centrality* and *positive degree centrality* respectively. These centralities evaluate how strong the local connectivity or influence of each node individually is.

In order to study the remaining centrality measures, we first need to highlight an important aspect of a distance metric. Distance is a value that represents how closely related two objects are, the lower the value, the closer

[5] Graph theorists refer to the degree centrality in unweighted graphs simply as *degree*, and in weighted graphs as the *weight* of the vertex.

those objects are[6]. In contrast, the higher partial correlation between two firms is, the more related they are. Therefore, we need to reverse the order of the partial correlations so the respective new values can be handled like a proper distance metric, where lower values correspond to closeness.

Closeness centrality of a node is defined as the inverse of the sum of its distances to all other nodes in the network, i.e.,

$$C_C(i) = \left[\sum_{j\neq i} d(i,j)\right]^{-1} = \frac{1}{\sum_{j\neq i} d(i,j)}. \tag{4.18}$$

Since this value is at most equal to $\frac{1}{N-1}$, then the normalized closeness centrality of the node i is

$$C_C^*(i) = (N-1)C_C(i). \tag{4.19}$$

On the same note, the *harmonic centrality* of a vertex is defined as

$$C_H(i) = \sum_{j\neq i} \frac{1}{d(i,j)}, \tag{4.20}$$

where $1/d(i,j) = 0$ if the distance between i and j is infinite. The *normalized harmonic centrality* of a node is

$$C_H^*(i) = \frac{1}{N-1} C_H(i). \tag{4.21}$$

Both, closeness and harmonic centralities, measure how close a node is to all remaining nodes and have quite similar behavior, the main difference

[6] To get into the mathematical theory behind metric spaces go to Willard 2012.

being that closeness centrality is not defined for disconnected graphs while harmonic centrality is. Both normalized versions lie in the real interval $[0, 1]$, where the closer these values are to 1, the closer the respective vertex is to the others.

Alternatively, the *betweenness centrality* of a node is defined as

$$C_B(i) = \sum_{s \neq i \neq t} \frac{\sigma_{st}(i)}{\sigma_{st}}, \tag{4.22}$$

where σ_{st} denote the number of distinct godesics from s to t, and $\sigma_{st}(i)$ is the number of those geodesics that contain the node i. And, the *normalized betweenness centrality* of a node is

$$C_B^*(i) = \frac{2}{(N-1)(N-2)} C_B(i). \tag{4.23}$$

In this case, we measure the importance of node i given its location within the topology of the network, in a sense, we are quantifying how essential is i to the connectivity of any pair of the remaining nodes, in other words, if i acts (or not) as a bridge that connects the other members of the graph.

Now, given $\mathbf{A}$ the adjacency matrix of the network, and λ the largest eigenvalue of $\mathbf{A}$, the *eigenvector centrality* of the vertex i, denoted $C_E(i)$, is the i-th entry of the eigenvector $\mathbf{x}$, which is the unique solution to the equation

$$\mathbf{A}\mathbf{x} = \lambda \mathbf{x}$$

such that x has only positive entries and $xx^\top = 1$, hence $C_E(i) = x_i$, where

[6] The existence of such solution is guaranteed by the Perron–Frobenius Theorem, see Horn and Johnson 2012

$\mathbf{x}^\top = (x_1\ x_2\ \cdots\ x_N)$. This centrality measures how important a node is in the network depending on its neighbors' importance.

4.4 Homophily

When analyzing a network, one can wonder if certain attributes of the vertices, or their combination, play a role in the existence of edges or the lack thereof within the network. For instance, in social networks, friendships generally tend to establish between people with similar characteristics (gender, age, beliefs, spoken language, etc.); by contrast, couples are prone to form between persons of the opposite gender on a dance floor. We can detect such behavior by measuring what is called *homophily*: to assess if there is a bias (in favor or against) on the number of links between nodes with similar characteristics.

To measure any network's bias in the distribution of edges towards one or more regions, we have to compare the relative number of edges inside such regions against the whole graph. Given the network G, and $X_1, X_2, \ldots, X_k$ disjoint subsets of vertices with size $n_1, n_2, \ldots, n_k$ respectively, we first compute the maximum possible number of edges such that both of its ends are in the same subset X_i, which is $\binom{n_i}{2}$ for each i. Then, we sum all of these values and divide the result by the maximum number of edges of the whole network, i.e, $\binom{N}{2}$, this quotient is called the *baseline homophily ratio* of the network G and its denoted by $h^*(G)$, in other words

$$h^*(G) = \binom{N}{2}^{-1} \sum_{i=1}^{k} \binom{n_i}{2} = \sum_{i=1}^{k} \frac{n_i(n_i-1)}{N(N-1)}.$$

Later, we compute the *homophily ratio* of the network G, denoted by $h(G)$, which is quotient of the total number of edges in the network whose ends are both in the same subset X_i to the total number of edges in the network, that is

$$h(G) = \sum_{i=1}^{k} \frac{m_i}{m(G)},$$

where m_i is the number of links with both ends in X_i.

When a network is constructed in such a way that each link has the same probability of forming despite the attributes of its endvertices, it is fair to expect that both ratios would be pretty close. So, whenever the homophily ratio is significantly greater than its baseline, then G is called *homophilic*, and when it is significantly lower it is said that G is *heterophilic*[7]. For example, in Figure 4.2 we can see two networks with opposite homophilic behavior. In both cases, the subsets of vertices considered are the same and colored red, blue, and green, respectively, so the baseline homophily is equal to $26/91 = 0.29$ for the two networks. On the other hand, the homophily ratios are $20/28 = 0.71$ and $6/38 = 0.16$ for the left and right networks, respectively.

Clearly, both ratios will almost surely differ in their values, so a statistical significance test is often used to quantify how significant their difference is. In our case, we will not use such a test since we will focus on how the difference of the homophily ratios is related to the strength of the relations of the network by considering a sequence of increasing cut-offs to the weight of the edges.

[7]Some authors refer to this as *inversed homophily*.

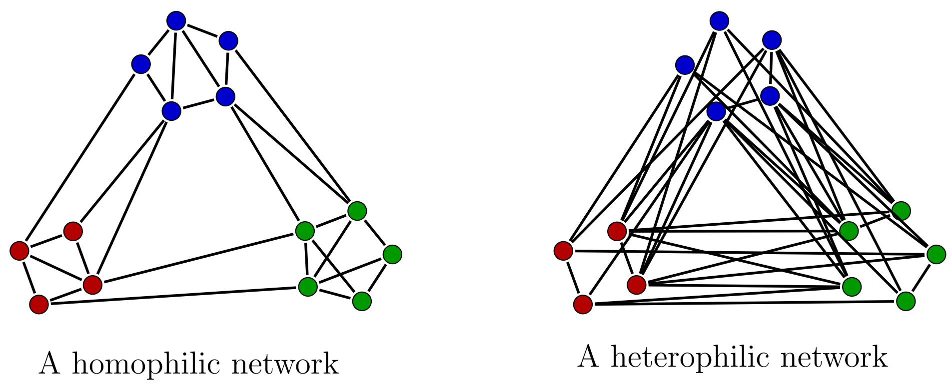

Figure 4.2: Examples of homophilic and heterophilic networks. In both cases three subsets of vertices are considered and marked with different colors.

4.5 Network Skeleton

To better understand and analyze a complex system, we often use different networks to represent the state of the system at different points in time, so at the end, we have a collection of networks that enable us to study the evolution of the system over time. Taking that into account, we define *dynamic network* as an ordered sequence of networks defined over the same set of vertices[8]. When working with weighted networks, we can interpret the weight of each link in a given moment as the strength of the relationship it represents at that particular point in time, and no matter how strong, some of these relations tend to appear and disappear over time. In contrast, another critical aspect to consider about any link is its resilience which does not consider its weight; instead, we are looking for edges whose presence is

[8]In general, the number of vertices is not set from the beginning since vertices can pop in and out of existence depending on the analyzed phenomenon; in our case, the set is fixed as we consider the same collection of firms for the whole period under study.

constant over time, leading us to the following definitions.

In a dynamic network, an edge is *resilient* if it appears in the network at every point during the studied period, i.e., in every network of the sequence. The set containing all resilient edges and their corresponding vertices form a network called the *skeleton* of its respective dynamic network. When dealing with weighted networks, we define the weight of each edge as the mean of the corresponding weights in the dynamic network. Figure 4.3 shows a dynamic network formed by three different networks labeled by day, and the respective network skeleton with their weights included.

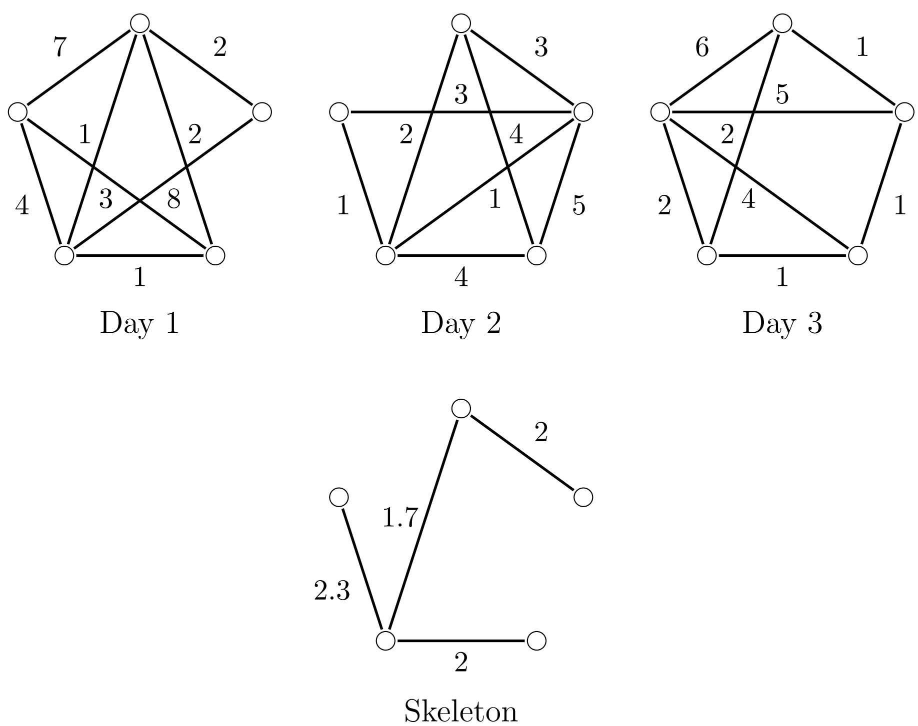

Figure 4.3: Skeleton of a dynamic network.

5 Results and Analysis

When analyzing the network characteristics, we considered the 1,201 days; additionally, we performed a study around the COVID-19 pandemic, where we considered four stages, Sans-COVID, Pre-COVID, During-COVID and Post-COVID, the corresponding periods are from January 2016 to October 2019, November 2019 to February 2020, March to June 2020, and July to September 2020. Throughout this thesis, we will refer to these stages as Sans, Pre, Dur, and Post, respectively.

From the cDCC-GARCH model, and after applying the GGM, we obtained data related to 1,201 days; from here, we can construct 1,201 individual networks that can be interpreted as daily pictures that allow us to see the state on any particular day; moreover, this also grants us a broader scope depicting the behavior of the dynamic network over time.

The data mentioned above contains negative and positive values, leading to data distortion or data loss in some instances (e.g., when adding values). For this reason, we take into account the following cases throughout this work:

- *Net* data, the original values, positive and negative.
- *Absolute* data, that is, the absolute value of original data.
- *Positive* data, i.e., only positive values within the data.

In order to achieve a better understanding of each network, we applied Fisher's transformation to increase the number of zeros in the adjacency matrix, considering a confidence level of 10%. This transformation led us to consider as zeros all those partial correlations between (-0.0558, 0.0558). Each network has 331 vertices representing the firms and 54,615 possible relations, i.e., its maximum number of edges.

While calculating the distances in the network, we encountered negative cycles when using the net data; therefore, there is no way to measure the distance for those values. Hence, it is necessary to consider only positive and absolute weights for calculating any distance-related parameter (radius, diameter, average distance, betweenness, closeness, and harmonic centralities). This way, we avoid the existence of negative cycles.

5.1 Global Measures

A first glimpse into the network structure can be made by analyzing the number of edges and their weights (Table 5.1). Over the 1,201 days, the mean number of edges in the network was 13,227 and always stayed between the 22.6% and 24.7% of the total possible edges (54,615). It is worth noticing that the number of positive weighted edges against the total is remarkably stable since it remained around the 54.7% during the whole period and deviating by no more than 0.57%, which implies that the numbers of negative and positive edges are closely related. This relation extends to their weights, where positive edges represent 56.8% with a maximum deviation of 0.62%. Hence negative and positive edges have a mirror behavior, as shown in Figure 5.1 where we plotted the aggregate weight against time.

Table 5.1: *Edge weight and edge count*

	Mean	Minimum	Maximum
Positive edges	7245.7	6818	7397
Negative edges	5981.8	5547	6145
Total edges	13227.5	12365	13504
Normalized total edges	0.242	0.226	0.247
Positive weights	615.6	574.6	627.2
Negative weights	-467.7	-482.3	-427.1
Total (absolute) weights	1083.3	1001.7	1107.7
% Positive edges	54.8	54.2	55.341
% Positive weight	56.8	56.4	57.443

Notes: Number of edges and their aggregated weight by type, positive and negative. *Source:* Author's calculations.

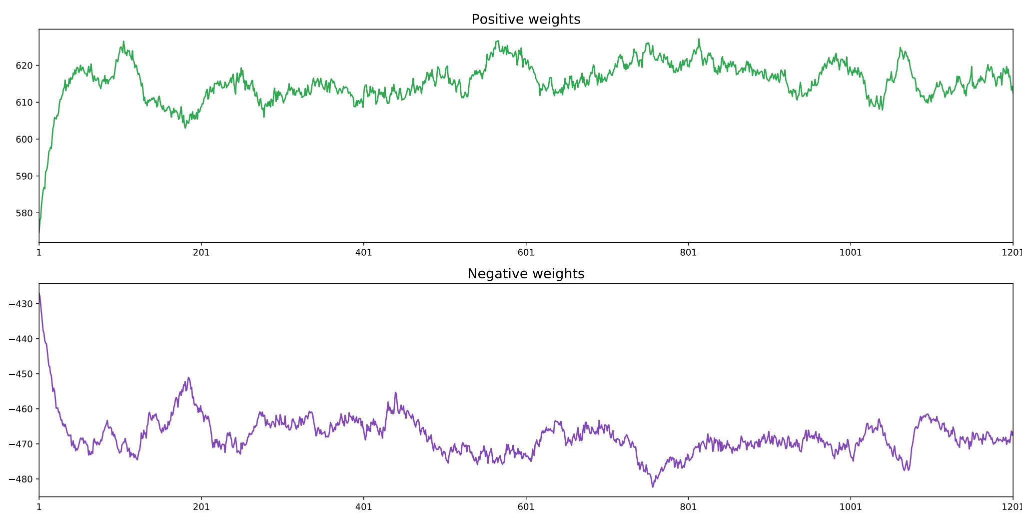

Figure 5.1: Weights of Positive and Negative Edges. *Source:* Author's calculations.

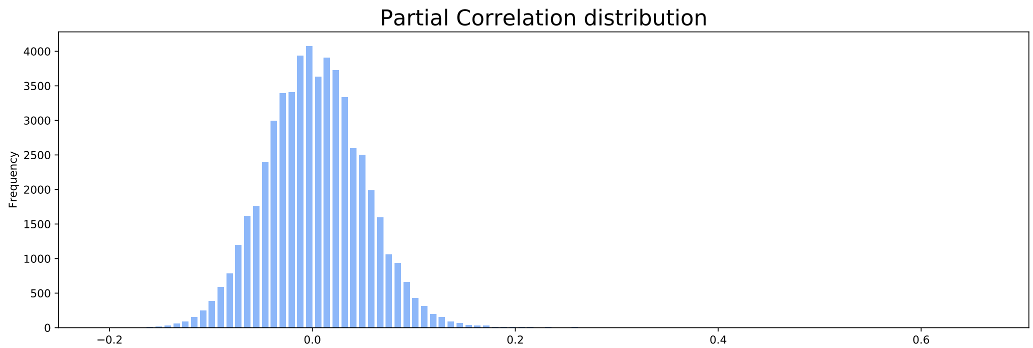

Figure 5.2: Partial correlation distribution. *Source:* Author's calculations.

Almost half of the relations in each network are negative, reaching their maximum magnitude at -0.24, as shown in Figure 5.2. This notably affects the net weights since they counterweight the strength of instability phenomenons. Therefore, given the described behavior of the edge weights, we can also appreciate that the positive weights and the absolute value of the weights have similar behavior, just transferred to a different scale, Figure A.2.

On the other hand, we can observe that before the beginning of the Pre period there is a meaningful shortage in the average path length. However, this decline was gradual since May 2018 and reached its lowest value in February 2019; again, in Dur period, there is a sudden increase followed by a sudden decay in the length of the shortest path, Figures A.3 and A.4. This behavior suggests that although there was no increase in connectedness, there was an inconstancy alternation in the intensity of existing relationships. In the network of positive values, we do not find a visible change in its behavior over time for the radius and diameter. In the network of absolute values, specifically the radius, a more pronounced peak is perceived just in the Dur dates.

On average, the positive and absolute networks have an average distance, radius, and diameter of 16.7, 20.8, and 25.8, and 18.5, 23.3, and 29.22, respectively, shown in Table 5.2. The diameter, radius, and average distance together give us a broader description of the network's topology.

Table 5.2: *Global Measures*

Network	Parameter	Mean	Min.	Max.
Abs	$\overline{d}(G)$	16.65	16.51	18.9
	$\mathrm{rad}(G)$	20.83	19.69	24.30
	$\mathrm{diam}(G)$	25.79	24.74	30.73
	$\overline{d}(G)$	18.53	18.36	21.66
Pos	$\mathrm{rad}(G)$	23.33	22.29	27.53
	$\mathrm{diam}(G)$	29.22	27.97	37.17

Notes: Absolute and positive network global parameters during 2016-2020.
Source: Author's calculations.

5.2 Local Measures

To analyze the centralities of the dynamic networks (absolute and positive), we took as a basis the average centrality per day of the degree, closeness, harmonic, betweenness, and eigenvector centralities. In the case of the degree centrality, we also calculated the net value.

Of the top 1 with highest centralities by industry, shown in Table 5.3, we noticed that three stick out, the Computers & Peripherals and Office Electronics (THQ), for three centralities: C_E^+, C_D^{net}, and C_D^+. The Semiconductors & Semiconductor Equipment (SEM) in both harmonic centralities and Paper

& Forest Products industries (FRP) in both betweenness centralities.

In the case of the top 1 by country, in Table 5.3, Spain excel for six of them (C_E^{abs}, C_D^{abs}, C_D^{pos}, C_C^{+}, C_H^{abs} and C_H^{+}) while Portugal in two (C_E^{+} and C_D^{net}), these two countries represent more than 3/4 of the firms with highest centralities.

Table 5.3: *Top 1 centralities, by industry and country*

	Industry		**Country**	
Centrality	Max.	Code	Max.	Code
C_E^{abs}	0.061	BLD	0.057	ES
C_E^{+}	0.064	THQ	0.059	PT
C_D^{net}	1.273	THQ	1.146	PT
C_D^{abs}	7.278	REX	6.932	ES
C_D^{+}	4.070	THQ	3.977	ES
C_C^{abs}	0.062	ALU	0.061	CH
C_C^{+}	0.057	COM	0.055	ES
C_H^{abs}	21.98	SEM	21.34	ES
C_H^{+}	20.24	SEM	19.34	ES
C_B^{abs}	0.005	FRP	0.004	FI
C_B^{+}	0.006	FRP	0.004	BE

Notes: Top 1 average centralities by industry and country from 2016-2020.
Source: Author's calculations.

Considering the positive and absolute networks, from the Top 20 of the highest centralities[1], only three and five firms, respectively, transmitted simultaneously positive and negative effects, look in Table 5.4. And from this only two, STERV.HE, and SSE.L, appear in the eleven rankings simultaneously.

[1] The comprehensive Top 20 highest centralities are in Tables: A.1, A.2, A.3, A.4, A.5, A.6, A.7, A.8, A.9, A.10, and A.11.

Taking into account the market capitalization by industry, the twelve most capitalized industries represent 59.81% and are 45.9% of the firms (Table A.12). On the other hand considering it by country, United Kingdom, France, Switzerland, and Germany represent 70.7% of market capitalization and 62.2% of the firms (Table A.16). We can notice that in both partitions, the countries or industries with the highest centralities are not precisely the most capitalized.

On the other hand, analyzing the network's connectedness again by its constituents, the United Kingdom connections remained unaffected in their number and their strength by the effect of the pandemic. France and Germany have a slight increase in number and strength of connections in the Pre and Dur periods. Austria was the country which strengthened its relations the most, although it has only one connection, more detail in Table A.17.

Additionally, we observe in Table A.17 that all but two countries have a standardized number of edges greater than the average per day for the whole network, 24.2%, which is a clear indication of homophilic behavior. This led us to review the number of connections between industries, look Table A.18, we took 12 companies, representing 50% of the index, and we noticed the same behavior.

Table 5.4: *Simultaneous effects of centralities in the Top 20*

	Industry		Country	
Centrality	Max.	Code	Max.	Code
C_E^{abs}	0.061	BLD	0.057	ES
C_E^{+}	0.064	THQ	0.059	PT
C_D^{net}	1.273	THQ	1.146	PT
C_D^{abs}	7.278	REX	6.932	ES
C_D^{+}	4.070	THQ	3.977	ES
C_C^{abs}	0.062	ALU	0.061	CH
C_C^{+}	0.057	COM	0.055	ES
C_H^{abs}	21.98	SEM	21.340	ES
C_H^{+}	20.24	SEM	19.340	ES
C_B^{abs}	0.005	FRP	0.004	FI
C_B^{+}	0.006	FRP	0.004	BE

Notes: Most relevant centralities simultaneously for positive and absolute values, respectively. *Source:* Author's calculations.

5.3 Homophily

To generate the homophily profile, we established an increasing sequence of cut-offs to obtain the links that represent the stronger relations between firms. It is worth mentioning that those cut-offs are to the absolute value of the edge weight. So, for instance, two links with weight 0.4 and -0.4 respectively represent equally strong relations although not the same kind of relations; this implies that the homophily profile of the net and absolute network are the same, regardless of the subsets of nodes considered. Also, we studied the homophily over two distinct partitions of the vertex set of the network: by country and by industry. In both cases, we calculated the homophily ratio for the 1,201 days of period.

Dividing the firms by country, we obtain a homophily baseline of 0.125 and the homophily ratio of the networks exhibited in Table 5.5; it is clear not only that each homophily index exceeds the baseline, but the homophily index is higher in each network, under stronger edges. Hence, once we reach a cut-off of 0.45, every existing link is between firms belonging to the same country for every daily network.

Table 5.5: *Homophily ratios by country.*

	Net/Abs			**Pos**		
Cut-offs[2]	Mean	Min	Max	Mean	Min	Max
0.05	0.149	0.145	0.153	0.192	0.187	0.197
0.1	0.214	0.201	0.229	0.290	0.271	0.308
0.15	0.469	0.433	0.512	0.528	0.486	0.568
0.2	0.670	0.621	0.718	0.674	0.626	0.723
0.25	0.745	0.703	0.779	0.745	0.703	0.779
0.3	0.755	0.714	0.816	0.755	0.714	0.816
0.35	0.814	0.778	0.852	0.814	0.778	0.852
0.4	0.947	0.857	1.0	0.947	0.857	1.0
0.45	1.0	1.0	1.0	1.0	1.0	1.0

Notes: The mean, minimum and maximum for the whole period of 1,201 days are presented for the net/absolute data on the left, and positive data on the right. *Source:* Author's calculations.

Now, considering the division of firms by the respective industry, we have a baseline homophily equal to 0.028 and, as in the previous case, all homophily ratios are above the baseline, and again, as the strength of the links we consider increases, the homophily increases as well, reaching full

[2]Recall that by using Fisher's transformation we applied a cut-off of 0.558 since the beginning, then the first cut-off of tables 5.5 and 5.6 correspond to all the edges in the studied networks.

homophily with a cut-off of 0.55 in every daily skeleton.

This implies that stronger relations tend to be established between firms that belong to the same country and industry.

For instance, this can be observed in Figures A.5 through A.8. A cut-off value equal to 0.3 was applied in these networks, i.e., only links between firms whose partial correlation was greater than or equal to 0.3 were drawn. In each figure, there are networks for the Pre, Dur, and Post periods where the color of a node corresponds to the country or industry that it belongs to, respectively.

Table 5.6: *Homophily ratios by industry.*

	Net/Abs			**Pos**		
Cut-offs[3]	Mean	Min	Max	Mean	Min	Max
0.05	0.051	0.049	0.053	0.083	0.079	0.087
0.1	0.141	0.131	0.160	0.217	0.204	0.242
0.15	0.554	0.519	0.611	0.633	0.584	0.683
0.2	0.843	0.802	0.876	0.848	0.809	0.876
0.25	0.869	0.831	0.897	0.869	0.831	0.897
0.3	0.892	0.846	0.929	0.892	0.846	0.929
0.35	0.888	0.875	0.900	0.888	0.875	0.900
0.4	0.904	0.800	0.944	0.904	0.800	0.944
0.45	0.905	0.889	0.917	0.905	0.889	0.917
0.5	0.945	0.833	1.0	0.945	0.833	1.0
0.55	1.0	1.0	1.0	1.0	1.0	1.0

Notes: The mean, minimum and maximum for the whole period of 1,201 days are presented for the net/absolute data on the left, and positive data on the right. *Source:* Author's calculations.

5.4 Skeleton

We consider the skeletons of each data type encompassing the whole time frame, we also construct the skeletons for each of the COVID related periods (Total, Sans, Pre, Dur, and Post) to examine if there is another piece of evidence about the impact of the pandemic onto the topology of the network.

When looking into the daily networks' average statistics (Table 5.7), we notice no particular change in its number of edges or its added weight. Even looking into the global measures of the skeletons of each period (Table 5.8), we cannot infer any trend or odd behavior due to the difference in the size among the time intervals since considering a skeleton of a larger time interval leads to a lower number of edges. We should keep in mind that an edge is part of the skeleton if and only if such edge is present in every daily network of the respective period.

Table 5.7: *Daily Networks – Edge Statistics*

		Total	Sans	Pre	Dur	Post
Net	Count	13227.5	13223.3	13273.8	13211.9	13255.9
	Weight	147.8	147.9	146.7	147.4	148.3
Abs	Count	13227.5	13223.3	13273.8	13211.9	13255.9
	Weight	1083.3	1083.1	1086.0	1081.7	1085.1
Pos	Count	7245.7	7245.2	7257.8	7230.5	7260.1
	Weight	615.6	615.5	616.4	614.6	616.7

Notes: Average by COVID Periods. *Source:* Author's calculations.

Since the Pre and Dur periods include precisely 84 days, we divided the Sans period into 84-day intervals (from March 2016 to February 2020). We compute the mean, standard deviation, minimum, and maximum of the first twelve uniformly divided periods, and by comparing these against the values of the Dur skeleton (Table 5.9), we can notice that the measures of the Dur period are above the maximum or below the observed minimum for the previous periods. In fact, the edge count and weight of the Dur period are higher than the corresponding maximum of the other periods. In contrast, all its others measures are lower than the respective minimum, with only one exception, the diameter of the absolute data.

Table 5.8: *Period Skeletons – Global Measures*

		Total	Sans	Pre	Dur	Post
	Edges					
Net	Count	2939.0	3073.0	6838.0	8160.0	8193.0
	Weight	102.81	103.38	135.27	140.00	135.76
Abs	Count	2939	3073	6838	8160	8193
	Weight	341.14	352.69	657.42	756.96	759.45
Pos	Count	1809	1880	3955	4650	4636
	Weight	221.98	228.03	396.35	448.48	447.60
	Distance					
Abs	$\overline{d}(G)$	18.90	18.81	17.36	17.07	17.05
	$\mathrm{rad}(G)$	24.30	24.00	21.98	21.03	21.16
	$\mathrm{diam}(G)$	30.73	30.86	27.57	27.66	26.45
Pos	$\overline{d}(G)$	21.66	21.52	19.44	19.07	19.08
	$\mathrm{rad}(G)$	27.53	27.33	23.95	23.74	23.92
	$\mathrm{diam}(G)$	37.17	37.52	30.99	29.62	30.27

Notes: The number of connections and their weight presented for the three kinds of data. Additionally, average distance, radius, and diameter for absolute and positive data. All of this for the COVID-related periods. *Source:* Author's calculations.

Table 5.9: *84-Day Skeletons – Global Measures*

		March 2016 to February 2020				
		Mean	Std Dev	Min	Max	Dur
	Edges					
	Count	6716.00	217.47	6349	7155	8160
Net	Weight	130.33	2.74	125.17	135.27	140.00
	W/C	0.019	0.001	0.018	0.020	0.017
	Count	6716.00	217.47	6349	7155	8160
Abs	Weight	649.01	18.38	619.82	687.20	756.96
	W/C	0.097	0.001	0.096	0.098	0.093
	Count	3864.83	111.39	3668	4063	4650
Pos	Weight	389.67	9.33	374.17	407.04	448.48
	W/C	0.101	0.001	0.100	0.102	0.096
	Distance					
	$\overline{d}(G)$	17.37	0.10	17.14	17.50	17.07
Abs	rad(G)	21.71	0.30	21.08	22.03	21.03
	diam(G)	27.59	0.34	26.96	28.12	27.66
	$\overline{d}(G)$	19.47	0.12	19.23	19.63	19.07
Pos	rad(G)	24.43	0.42	23.92	25.05	23.74
	diam(G)	31.37	0.73	30.53	33.45	29.62

Notes: We show the edge count, edge weight, and ratio (weight over count), radius, diameter, and average distance for each correspondent network kind. We have the mean, standard deviation, minimum and maximum for the first twelve 84-day skeletons in the first four columns. At the same time, the last column shows the respective values for the last period, Dur, which goes from March to June 2020. *Source:* Author's calculations.

So, even when there is no remarkable change in the edge count and weight of the overall network (Table 5.7), it is noteworthy that the number of resilient edges in the Dur period is over 14% higher than the maximum in the previous 84-Day Skeletons intervals (Table 5.9), i.e., the number of relations did not substantially change, but the stability of their relations increased.

While studying the centralities of the skeletons corresponding to the COVID periods, we observe two types of behavior. On the one hand, degree and eigenvector centralities rankings did not maintain much stability, while closeness, harmonic, and betweenness were pretty stable during all periods.

As we can see in Table 5.10, no firm simultaneously appears in the top 20 of the three types of data. Until we consider the top 30 rankings, one firm accomplishes the simultaneous occurrence, namely, CABK.MC, whose net degree centralities are 1.24, 1.32, 1.5, 1.74, and 1.62 for the Total, Sans, Pre, Dur and Post periods, respectively.

Similarly, no firm has an eigenvector centrality that allow it to appear in all top 20 rankings (Table 5.11), only GRF.MC is included among the top 30 firms in every period and every type of data.

Table 5.10: *Simultaneous Top 20 (Degree Centrality)*

	Ticker	Total	Sans	Pre	Dur	Post
Net	BN.PA	1.93	1.93	1.76	2.38	1.98
	SU.PA	1.59	1.68	1.83	1.76	2.14
Abs	CABK.MC	3.96	4.04	6.04	7.17	6.30
	CFR.SW	3.38	3.47	5.52	6.45	6.02
	SSE.L	3.32	3.49	5.35	6.83	6.72
Pos	CABK.MC	2.60	2.68	3.77	4.45	3.96
	STERV.HE	2.47	2.55	3.41	3.65	3.64
	SSE.L	2.16	2.16	3.48	4.31	4.41
	ATCO-A.ST	2.06	2.14	3.24	3.59	3.57

Notes: Degree centrality top 20 of every period for net, absolute and positive data. *Source:* Author's calculations.

Table 5.11: *Simultaneous Top 20 (Eigenvector Centrality)*

	Ticker	Total	Sans	Pre	Dur	Post
Abs	ATL.MI	0.090	0.091	0.074	0.089	0.073
	PGHN.SW	0.085	0.081	0.075	0.075	0.072
	SSE.L	0.084	0.084	0.072	0.080	0.080
Pos	BN.PA	0.119	0.113	0.074	0.077	0.079
	WEIR.L	0.084	0.086	0.082	0.073	0.081

Notes: Eigenvector centrality Top 20 of every period for absolute and positive data. *Source:* Author's calculations.

In contrast, five firms, BBVA.MC, CABK.MC, CFR.SW, GLE.PA and SSE.L, appear in the Top 10 of the closeness centrality ranking of every period and every data type (see Table 5.12). For the harmonic centrality, six firms consistently appear in all top 10 rankings, namely, CFR.SW, BBVA.MC, CABK.MC, GLE.PA, STERV.HE and UPM.HE (Table 5.13). Moreover, BBVA.MC, CABK.MC, CFR.SW, CSGN.SW, and STERV.HE are always present in the top 10 of betweenness centrality despite data type and period (Table 5.14).

So three firms, BBVA.MC, CABK.MC, and CFR.SW accomplished being in each top 10 rankings of three centralities of every skeleton by period.

Table 5.12: *Simultaneous Top 10 (Closeness Centrality)*

	Ticker	Total	Sans	Pre	Dur	Post
Abs	CFR.SW	0.061	0.061	0.065	0.066	0.065
	BBVA.MC	0.061	0.061	0.064	0.065	0.065
	CABK.MC	0.060	0.060	0.064	0.066	0.065
	SSE.L	0.059	0.060	0.063	0.065	0.064
	UHR.SW	0.059	0.059	0.063	0.063	0.063
	GLE.PA	0.059	0.059	0.063	0.064	0.064
Pos	BBVA.MC	0.055	0.055	0.058	0.060	0.059
	CABK.MC	0.054	0.054	0.058	0.059	0.058
	STERV.HE	0.053	0.053	0.058	0.058	0.057
	CSGN.SW	0.053	0.054	0.057	0.058	0.058
	GLE.PA	0.053	0.053	0.057	0.058	0.057
	CFR.SW	0.052	0.052	0.057	0.058	0.058
	SSE.L	0.052	0.052	0.057	0.058	0.058

Notes: Closeness Centrality Top 10 of every period for absolute and positive data types. *Source:* Author's calculations.

Table 5.13: *Simultaneous Top 10 (Harmonic Centrality)*

	Ticker	Total	Sans	Pre	Dur	Post
Abs	CFR.SW	22.00	22.10	23.19	23.43	23.25
	BBVA.MC	21.58	21.62	22.63	23.03	22.98
	CABK.MC	21.57	21.60	22.87	23.40	23.02
	UPM.HE	21.22	21.25	22.79	22.73	22.50
	UHR.SW	21.13	21.19	22.20	22.43	22.47
	STERV.HE	21.06	21.17	22.69	22.55	22.36
	SSE.L	21.06	21.18	22.18	22.75	22.51
	GLE.PA	21.00	21.01	22.06	22.70	22.45
Pos	BBVA.MC	19.74	19.76	20.76	21.25	20.96
	CABK.MC	19.38	19.42	20.56	21.03	20.44
	STERV.HE	19.31	19.42	20.83	20.88	20.55
	CSGN.SW	19.17	19.34	20.38	20.62	20.49
	CFR.SW	19.02	19.06	20.61	20.77	20.69
	GLE.PA	18.79	18.81	20.01	20.44	20.29
	UPM.HE	18.74	18.79	20.47	20.51	20.19

Notes: Harmonic Centrality Top 10 of every period for absolute and positive data types. *Source:* Author's calculations.

Table 5.14: *Simultaneous Top 10 (Betweenness Centrality)*

	Ticker	Total	Sans	Pre	Dur	Post
Abs	CABK.MC	0.017	0.017	0.012	0.013	0.012
	CFR.SW	0.016	0.016	0.012	0.011	0.009
	BBVA.MC	0.014	0.013	0.009	0.009	0.009
	CSGN.SW	0.014	0.014	0.009	0.008	0.008
	UPM.HE	0.013	0.012	0.010	0.009	0.009
	STERV.HE	0.012	0.012	0.010	0.008	0.008
Pos	BBVA.MC	0.022	0.020	0.012	0.013	0.012
	CABK.MC	0.021	0.021	0.014	0.014	0.012
	STERV.HE	0.020	0.020	0.015	0.013	0.012
	SSE.L	0.019	0.018	0.012	0.012	0.012
	CSGN.SW	0.019	0.020	0.012	0.011	0.010
	BAS.DE	0.017	0.016	0.011	0.010	0.012
	CFR.SW	0.016	0.015	0.013	0.011	0.010

Notes: Betweenness Centrality Top 10 of every period for absolute and positive data types. *Source:* Author's calculations.

Finally, as in the case of daily networks in Section 5.3, we observed that the stronger ties in the network have homophilic behavior since the homophilic ratios are greater in every instance to the respective homophilic baselines of 0.125 for countries and 0.028 for industries, and when taking different thresholds for edge strength we observe that the homophilic ratio also increased as the cut-off also increased (see Figures A.9 and A.10). Moreover, by comparing the homophily ratios of skeletons and daily networks (Tables 5.5 and 5.6), we observed that skeletons always have homophily ratios greater than the mean of their respective daily networks. In fact, when considering the partition by industries, the homophily in the skeletons exceeds the maximum homophily of the daily networks for each cut- off. Therefore, we can say that resilient edges tend to be more homophilic; in other words, stable relations are more likely to form when firms share the same country and industry.

Table 5.15: *Homophily ratios over the skeletons*

	Country		**Industry**	
Cut-offs	Net/Abs	Pos	Net/Abs	Pos
0.05	0.199	0.269	0.114	0.180
0.10	0.227	0.307	0.163	0.244
0.15	0.488	0.540	0.604	0.674
0.20	0.692	0.692	0.850	0.850
0.25	0.758	0.758	0.871	0.871
0.30	0.750	0.750	0.900	0.900
0.35	0.815	0.815	0.889	0.889
0.40	1.0	1.0	0.929	0.929
0.45	1.0	1.0	0.909	0.909
0.50	1.0	1.0	1.0	1.0

Source: Author's calculations.

6 Conclusions

We analyzed the network's topology derived from the relationships among the companies that constitute the S&P 350 Europe index, using their adjusted closing prices from January 2016 to September 2020. For this, we calculated local and global parameters of the network. The analysis of centralities was carried out through two scenarios, first considering daily networks and second using the skeletons. On the first one, only two firms were found simultaneously in the top 20 of each of the eleven centralities calculated, so these firms are the ones that best transmitted positive and negative effects during the whole period. These are Scottish & Southern Energy (SSE.L) and Stora Enso OYJ R. (STERV.H.). These firms are from the Paper & Forest Products and Electric Utilities industries, and they are located in Finland and the United Kingdom, respectively. On the second scenario, for the degree and eigenvector centralities, no firms were simultaneously present on the top 20 rankings, indicating a lack of stability, but at the same time, closeness, harmonic, and betweenness were pretty stable during all periods, and three firms, accomplished to appear simultaneously in each top 10 rankings. These firms are Banco Bilbao Vizcaya Argentaria S.A. (BBVA.MC) in Spain, CaixaBank (CABK.MC) in Spain, and Compagnie Financière Richemont S.A. (CFR.SW) from Switzerland. The first two are from the bank industry and the third from Textiles, Apparel & Luxury Goods.

Placing the companies with the highest centralities serves to complement the company's risk profile and locate the systemic risk entities. Finding them allows the corresponding authorities to regulate them.

Using the 84-day skeleton construction, we detected an increase of 20% over the number of resilient relationships during the COVID-19 pandemic, while the total number of edges do not have a similar change. However, we could not conclude whether there was a significant change, nor in the number of edges, nor in the centralities' value over time, since some robustness test is needed for that purpose, and this was beyond our reach for a matter of time.

The financial network turned out to be highly homophilic, and in fact, a direct relationship between the partial correlation coefficient and the homophilic ratio was discovered, where the stronger relations tend to be established between firms that belong to the same country and industry. On the same note, homophily ratios of the skeletons proved to be greater than in the daily networks, which suggests resilient relations have a larger proclivity to be homophilic than unstable ones.

Additionally, for further study:

- Is homophily present in other stock indices networks?
- Although average distance, radius, and diameter help us better understand the power needed to be exerted over the network to trigger a cascade effect, the fact that (in this case) the radius is always greater than the average distance makes us wonder whether an analysis of average eccentricities would be more useful for systemic risk analysis than the average distance, leaving this topic open for further studies.
- The estimation of the clustering coefficient could be helpful to mea-

sure the density of the neighbourhood of the vertices and the graph, complementing the topological analysis.

- A skeleton generalization could be made, allowing flexibility in the absence of connections, with an α, such that $0 \leq \alpha \leq 1$, for instance, in this thesis, we are considering that edges should always be present in the period under study to belong to the skeleton, so we are using an α of zero. An alpha of one would be if we consider as a skeleton the union of all the networks in the period.

- Derive causal relationships between firms since we cannot derive them with the current study, given that we constructed an undirected graph.

A Appendix

A.1 Radius versus Average Path Length

The graphs shown below are examples where radius and average distance hold different inequality outcomes. In each of them the top vertex can reach any other vertex in at most $\mathrm{rad}(G_i)$ steps for $i = 1, 2, 3$.

$$1 = \mathrm{rad}(G_1) < \overline{d}(G_1) = 1.1$$

$$2 = \mathrm{rad}(G_2) > \overline{d}(G_2) = 1.5$$

$$2 = \mathrm{rad}(G_3) = \overline{d}(G_3) = 2$$

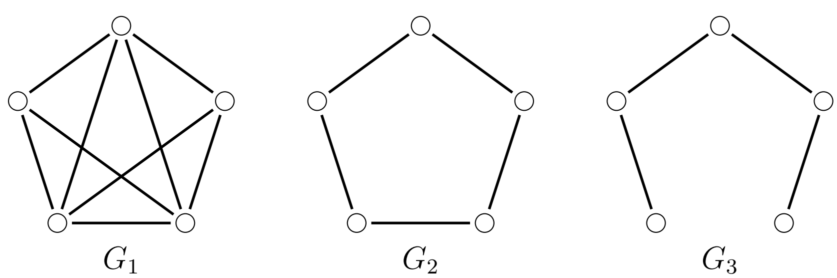

Figure A.1: Graphs where its radius and average distance have different order relationships.

A.2 Tables and Figures

Tables and figures appear in this section in the same order they were mentioned in the main text.

From Section 5.1

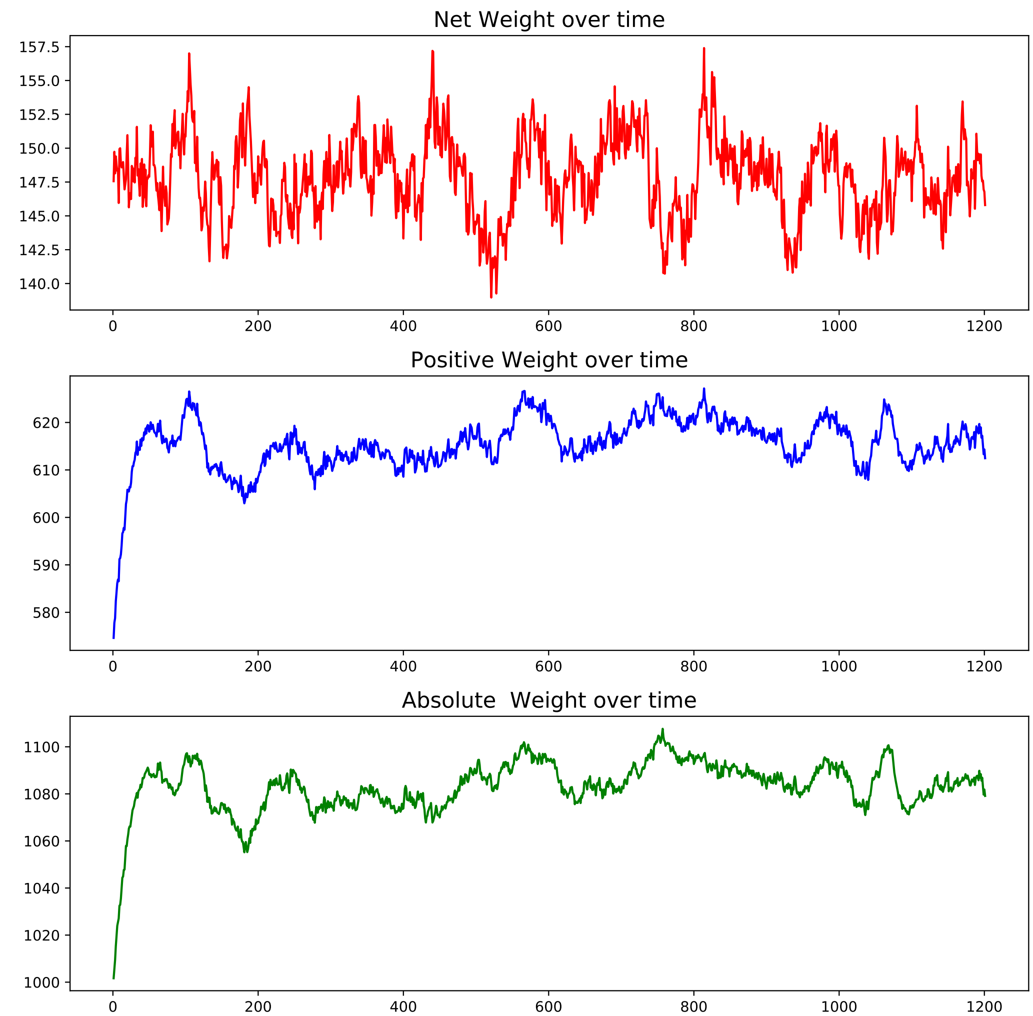

Figure A.2: Weights over time. Notice there is no change in the behavior of net weight, positive weight, and absolute weight in the COVID related periods. *Source:* Author's calculations.

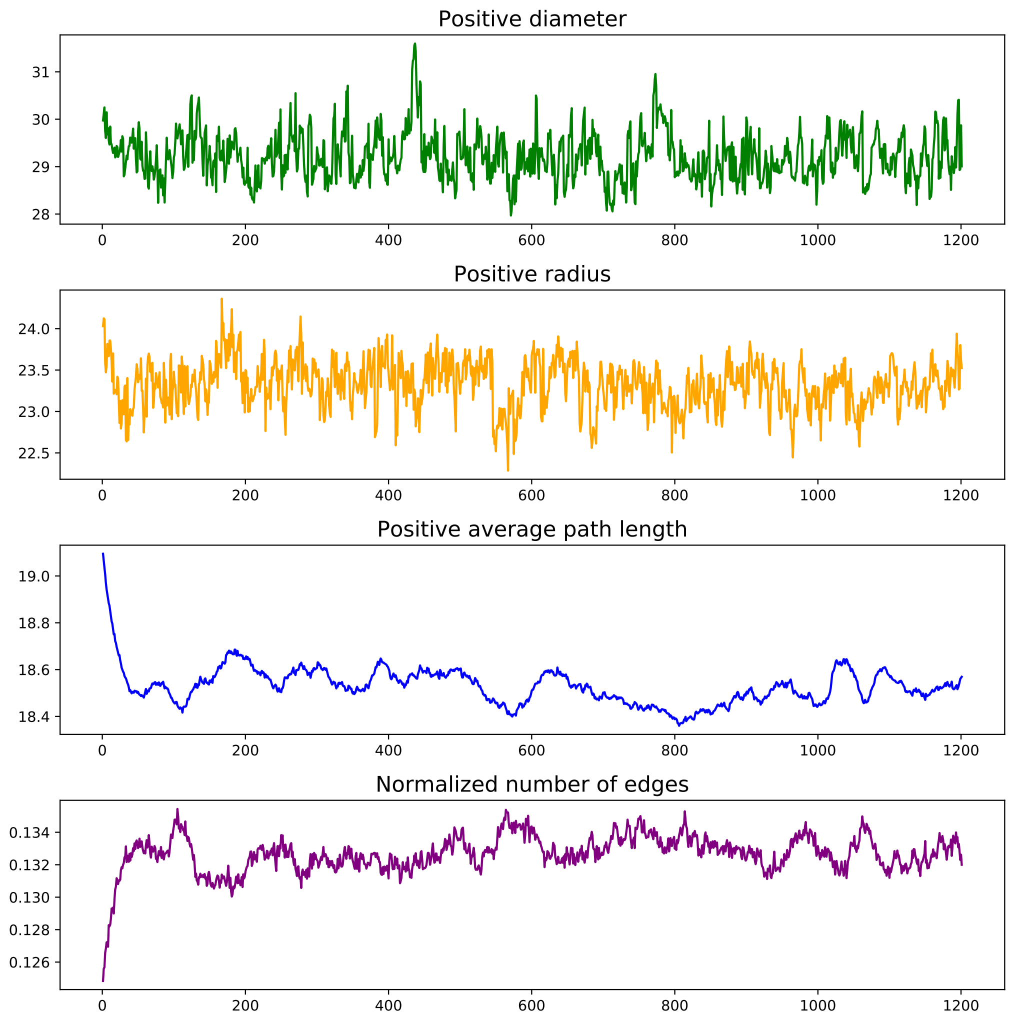

Figure A.3: Global measures over time. Diameter, radius, average distance, and the normalized number of edges, where positive values are considered. *Source:* Author's calculations.

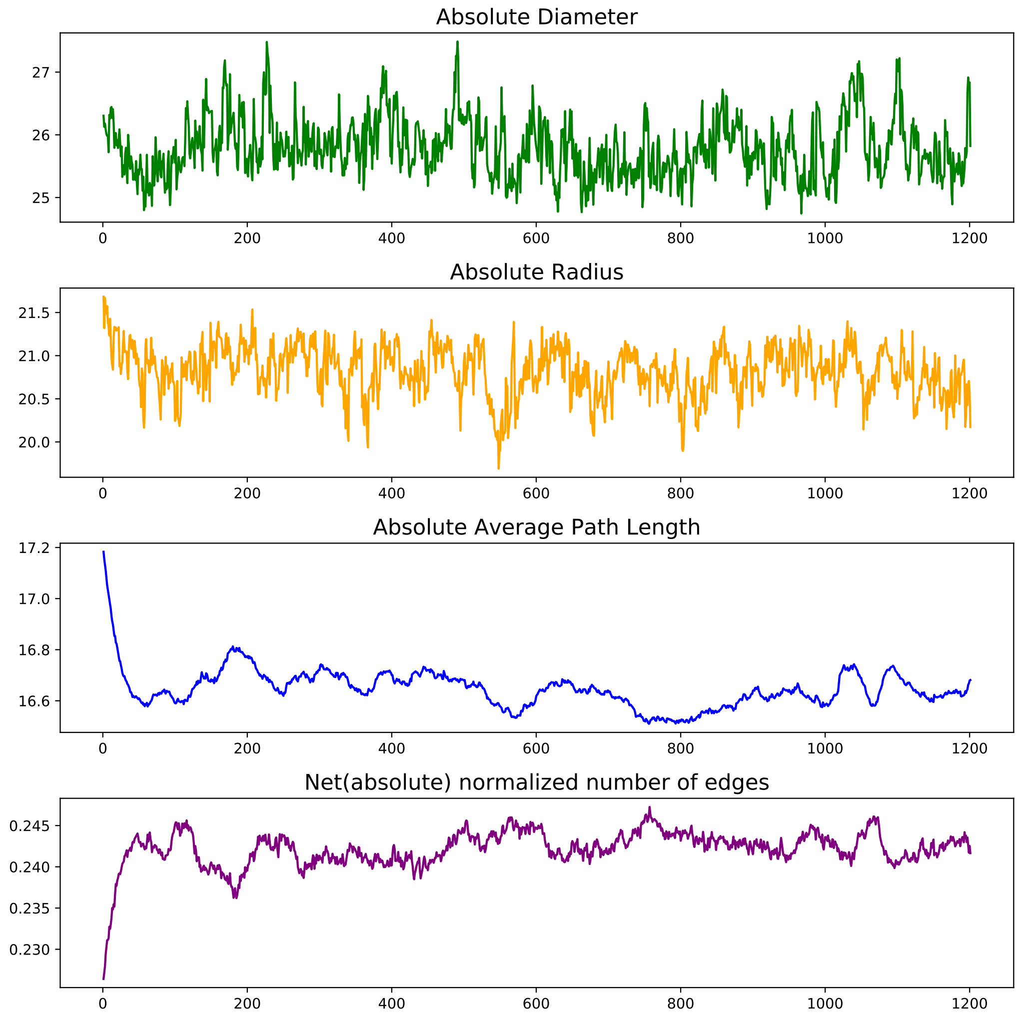

Figure A.4: Global measures over time. Diameter, radius, average distance, and the normalized number of edges, where absolute values are considered. Notice that the normalized number of edges is the same for the net scenario. *Source:* Author's calculations.

From Section 5.2

Table A.1: *Average net degree centrality C_D^{net} - 2016-2020*

Ticker	Industry	Num. Edges	C_D^{net}	ISO Code	Market Cap. %
INVE-B.ST	FBN	225	1.956	SE	0.240
BN.PA	FOA	230	1.787	FR	0.548
SN.L	MTC	212	1.779	GB	0.209
SU.PA	ELQ	214	1.769	FR	0.576
LEG.DE	REA	205	1.768	DE	0.078
CBK.DE	BNK	214	1.767	DE	0.075
AC.PA	TRT	222	1.697	FR	0.122
ZURN.SW	INS	233	1.696	CH	0.595
WEIR.L	IEQ	230	1.669	GB	0.050
ACA.PA	BNK	229	1.582	FR	0.403
CSGN.SW	FBN	218	1.558	CH	0.333
CABK.MC	BNK	227	1.557	ES	0.181
STERV.HE	FRP	249	1.551	FI	0.086
SAF.PA	ARO	235	1.550	FR	0.609
PSN.L	HOM	214	1.531	GB	0.109
OR.PA	COS	227	1.510	FR	1.590
SY1.DE	CHM	218	1.471	DE	0.137
SSE.L	ELC	229	1.460	GB	0.190
INF.L	PUB	202	1.452	GB	0.137
ORA.PA	TLS	217	1.439	FR	0.376

Notes: The twenty firms with most local influence, considering net degree Centrality. The number of edges is representing the average number of edges during the whole period 2016-2020. *Source:* S&P Global and author's calculations.

Table A.2: *Average absolute degree centrality (C_D^{abs}), 2016-2020*

Ticker	Industry	Num. Edges	C_D^{abs}	ISO Code	Market Cap. %
ATL.MI	TRA	241	8.810	IT	0.186
SSE.L	ELC	229	8.700	GB	0.190
TUI1.DE	TRT	236	8.696	DE	0.072
STERV.HE	FRP	249	8.689	FI	0.086
CABK.MC	BNK	227	8.606	ES	0.181
CFR.SW	TEX	228	8.583	CH	0.395
LR.PA	ELQ	226	8.320	FR	0.208
BBVA.MC	BNK	232	8.277	ES	0.359
DGE.L	BVG	236	8.272	GB	1.052
BOL.ST	MNX	232	8.191	SE	0.070
AGS.BR	INS	234	8.130	BE	0.113
BRBY.L	TEX	235	8.122	GB	0.116
KNIN.SW	TRA	217	8.086	CH	0.195
SOLB.BR	CHM	238	8.072	BE	0.118
LHN.SW	COM	232	8.028	CH	0.329
UPM.HE	FRP	222	7.963	FI	0.178
EN.PA	CON	236	7.948	FR	0.152
PGHN.SW	REA	226	7.938	CH	0.236
ASML.AS	SEM	233	7.891	NL	1.211
HNR1.DE	INS	225	7.886	DE	0.225

Notes: The twenty firms with most local influence, considering absolute degree centrality. The number of edges is representing the average number of edges during the whole period 2016-2020. *Source:* S&P Global and author's calculations.

Table A.3: *Average positive degree centrality (C_D^+), 2016-2020*

Ticker	Industry	Num. Edges	C_D^+	ISO Code	Market Cap. %
STERV.HE	FRP	126	5.12	FI	0.086
CABK.MC	BNK	113	5.082	ES	0.181
SSE.L	ELC	118	5.08	GB	0.19
INVE-B.ST	FBN	119	4.8	SE	0.24
CFR.SW	TEX	116	4.778	CH	0.395
WEIR.L	IEQ	126	4.74	GB	0.05
ATL.MI	TRA	127	4.711	IT	0.186
BRBY.L	TEX	121	4.679	GB	0.116
ZURN.SW	INS	119	4.665	CH	0.595
BBVA.MC	BNK	114	4.642	ES	0.359
BN.PA	FOA	115	4.628	FR	0.548
LAND.L	REA	118	4.624	GB	0.095
OR.PA	COS	112	4.582	FR	1.59
ATCO-A.ST	IEQ	107	4.576	SE	0.323
LR.PA	ELQ	119	4.554	FR	0.208
CPG.L	REX	116	4.552	GB	0.385
HNR1.DE	INS	114	4.541	DE	0.225
KNIN.SW	TRA	111	4.537	CH	0.195
BARC.L	BNK	121	4.535	GB	0.393
TUI1.DE	TRT	125	4.533	DE	0.072

Notes: The twenty firms with most local influence, considering positive degree centrality. The number of edges is representing the average number of edges during the whole period 2016-2020. *Source:* S&P Global and author's calculations.

Table A.4: *Average absolute closeness centrality (C_C^{abs}), 2016-2020*

Ticker	Industry	Num. Edges	C_C^{abs}	ISO Code	Market Cap. %
CFR.SW	TEX	228	0.067	CH	0.395
BBVA.MC	BNK	232	0.066	ES	0.359
CABK.MC	BNK	227	0.066	ES	0.181
SSE.L	ELC	229	0.066	GB	0.19
UPM.HE	FRP	222	0.065	FI	0.178
UHR.SW	TEX	232	0.065	CH	0.083
STERV.HE	FRP	249	0.065	FI	0.086
GLE.PA	INS	241	0.065	FR	0.284
MUV2.DE	INS	213	0.064	DE	0.41
TUI1.DE	TRT	236	0.064	DE	0.072
NG.L	MUW	225	0.064	GB	0.453
ALV.DE	INS	221	0.064	DE	0.985
ATL.MI	TRA	241	0.064	IT	0.186
LLOY.L	BNK	217	0.064	GB	0.561
LHN.SW	COM	232	0.064	CH	0.329
HNR1.DE	INS	225	0.064	DE	0.225
DGE.L	BVG	236	0.064	GB	1.052
CSGN.SW	FBN	218	0.064	CH	0.333
ATCO-A.ST	IEQ	217	0.064	SE	0.323
MC.PA	TEX	220	0.064	FR	2.282

Notes: The twenty firms with the highest closeness centrality, considering absolute values. The number of edges is representing the average number of edges during the whole period 2016-2020. *Source:* S&P Global and author's calculations.

Table A.5: *Average positive closeness centrality (C_C^+), 2016-2020*

Ticker	Industry	Num. Edges	C_C^+	ISO Code	Market Cap. %
BBVA.MC	BNK	114	0.06	ES	0.359
STERV.HE	FRP	126	0.06	FI	0.086
CABK.MC	BNK	113	0.06	ES	0.181
CFR.SW	TEX	116	0.06	CH	0.395
UPM.HE	FRP	109	0.059	FI	0.178
CSGN.SW	FBN	105	0.059	CH	0.333
GLE.PA	INS	127	0.059	FR	0.284
SSE.L	ELC	118	0.059	GB	0.19
MUV2.DE	INS	109	0.058	DE	0.41
UHR.SW	TEX	123	0.058	CH	0.083
NG.L	MUW	116	0.058	GB	0.453
INVE-B.ST	FBN	119	0.058	SE	0.24
LHN.SW	COM	118	0.058	CH	0.329
ATCO-A.ST	IEQ	107	0.058	SE	0.323
IFX.DE	SEM	106	0.058	DE	0.275
HNR1.DE	INS	114	0.058	DE	0.225
DGE.L	BVG	120	0.058	GB	1.052
BNP.PA	BNK	107	0.058	FR	0.711
SAN.MC	BNK	101	0.058	ES	0.67
ASML.AS	SEM	121	0.057	NL	1.211

Notes: The twenty firms with the highest closeness centrality, considering positive values. The number of edges is representing the average number of edges during the whole period 2016-2020. *Source:* S&P Global and author's calculations.

Table A.6: *Average absolute harmonic centrality (C_H^{abs}), 2016-2020*

Ticker	Industry	Num. Edges	C_H^{abs}	ISO Code	Market Cap. %
CFR.SW	TEX	228	23.896	CH	0.395
CABK.MC	BNK	227	23.422	ES	0.181
BBVA.MC	BNK	232	23.213	ES	0.359
STERV.HE	FRP	249	23.182	FI	0.086
UPM.HE	FRP	222	23.179	FI	0.178
SSE.L	ELC	229	22.985	GB	0.19
UHR.SW	TEX	232	22.906	CH	0.083
GLE.PA	INS	241	22.715	FR	0.284
CSGN.SW	FBN	218	22.655	CH	0.333
ALV.DE	INS	221	22.61	DE	0.985
DGE.L	BVG	236	22.549	GB	1.052
TUI1.DE	TRT	236	22.513	DE	0.072
HNR1.DE	INS	225	22.484	DE	0.225
NG.L	MUW	225	22.384	GB	0.453
LAND.L	REA	232	22.381	GB	0.095
MC.PA	TEX	220	22.375	FR	2.282
IFX.DE	SEM	214	22.345	DE	0.275
ATCO-A.ST	IEQ	217	22.344	SE	0.323
VNA.DE	REA	222	22.341	DE	0.282
MUV2.DE	INS	213	22.314	DE	0.41

Notes: The twenty firms with the highest harmonic centrality, considering absolute values. The number of edges is representing the average number of edges during the whole period 2016-2020. *Source:* S&P Global and author's calculations.

Table A.7: *Average positive harmonic centrality (C_H^+), 2016-2020*

Ticker	Industry	Num. Edges	C_H^+	ISO Code	Market Cap. %
STERV.HE	FRP	126	21.394	FI	0.086
BBVA.MC	BNK	114	21.361	ES	0.359
CFR.SW	TEX	116	21.306	CH	0.395
CABK.MC	BNK	113	21.112	ES	0.181
UPM.HE	FRP	109	20.954	FI	0.178
CSGN.SW	FBN	105	20.911	CH	0.333
SSE.L	ELC	118	20.891	GB	0.19
IFX.DE	SEM	106	20.678	DE	0.275
GLE.PA	INS	127	20.641	FR	0.284
HNR1.DE	INS	114	20.536	DE	0.225
LAND.L	REA	118	20.516	GB	0.095
UHR.SW	TEX	123	20.5	CH	0.083
MUV2.DE	INS	109	20.493	DE	0.41
SAN.MC	BNK	101	20.4	ES	0.67
INVE-B.ST	FBN	119	20.363	SE	0.24
ASML.AS	SEM	121	20.341	NL	1.211
ALV.DE	INS	122	20.305	DE	0.985
NG.L	MUW	116	20.301	GB	0.453
LLOY.L	BNK	111	20.298	GB	0.561
ATCO-A.ST	IEQ	107	20.297	SE	0.323

Notes: The twenty firms with the highest harmonic centrality, considering positive values. The number of edges is representing the average number of edges during the whole period 2016-2020. *Source:* S&P Global and author's calculations.

Table A.8: *Average absolute eigenvector centrality (C_E^{abs}), 2016-2020*

Ticker	Industry	Num. Edges	C_E^{abs}	ISO Code	Market Cap. %
ATL.MI	TRA	241	0.07	IT	0.186
EN.PA	CON	236	0.068	FR	0.152
BRBY.L	TEX	235	0.068	GB	0.116
TUI1.DE	TRT	236	0.068	DE	0.072
STERV.HE	FRP	249	0.068	FI	0.086
LHN.SW	COM	232	0.067	CH	0.329
SSE.L	ELC	229	0.067	GB	0.19
BOL.ST	MNX	232	0.066	SE	0.07
SPX.L	IEQ	236	0.066	GB	0.084
LR.PA	ELQ	226	0.066	FR	0.208
SCR.PA	INS	224	0.065	FR	0.075
WEIR.L	IEQ	230	0.065	GB	0.05
EXPN.L	PRO	233	0.065	GB	0.316
RSA.L	INS	218	0.064	GB	0.074
PGHN.SW	REA	226	0.064	CH	0.236
BBVA.MC	BNK	232	0.064	ES	0.359
KNIN.SW	TRA	217	0.064	CH	0.195
DGE.L	BVG	236	0.064	GB	1.052
MONC.MI	TEX	228	0.064	IT	0.112
SOLB.BR	CHM	238	0.063	BE	0.118

Notes: The twenty firms with the highest eigenvector centrality, considering absolute values. The number of edges is representing the average number of edges during the whole period 2016-2020. *Source:* S&P Global and author's calculations.

Table A.9: *Average positive eigenvector centrality (C_E^+), 2016-2020*

Ticker	Industry	Num. Edges	C_E^+	ISO Code	Market Cap. %
BRBY.L	TEX	121	0.071	GB	0.116
WEIR.L	IEQ	126	0.07	GB	0.05
TUI1.DE	TRT	125	0.069	DE	0.072
ATL.MI	TRA	127	0.069	IT	0.186
LR.PA	ELQ	119	0.069	FR	0.208
SSE.L	ELC	118	0.067	GB	0.19
REP.MC	OGX	110	0.066	ES	0.241
EN.PA	CON	124	0.066	FR	0.152
EXPN.L	PRO	118	0.066	GB	0.316
SDR.L	FBN	127	0.066	GB	0.096
TEP.PA	PRO	119	0.065	FR	0.138
STERV.HE	FRP	126	0.065	FI	0.086
AMS.MC	TSV	118	0.065	ES	0.34
INVE-B.ST	FBN	119	0.065	SE	0.24
HM-B.ST	RTS	124	0.065	SE	0.287
BN.PA	FOA	115	0.065	FR	0.548
CBK.DE	BNK	101	0.065	DE	0.075
KNIN.SW	TRA	111	0.065	CH	0.195
FGR.PA	CON	119	0.064	FR	0.108
TEF.MC	TLS	124	0.064	ES	0.35

Notes: The twenty firms with the highest eigenvector centrality, considering positive values. The number of edges is representing the average number of edges during the whole period 2016-2020. *Source:* S&P Global and author's calculations.

Table A.10: *Average absolute betweenness centrality (C_B^{abs}), 2016-2020*

Ticker	Industry	Num. Edges	C_B^{abs}	ISO Code	Market Cap. %
AGS.BR	INS	234	0.007	BE	0.113
ALV.DE	INS	221	0.007	DE	0.985
BBVA.MC	BNK	232	0.007	ES	0.359
BAS.DE	CHM	207	0.007	DE	0.669
CABK.MC	BNK	227	0.01	ES	0.181
CSGN.SW	FBN	218	0.007	CH	0.333
DGE.L	BVG	236	0.006	GB	1.052
EZJ.L	AIR	233	0.007	GB	0.072
HNR1.DE	INS	225	0.006	DE	0.225
INVE-B.ST	FBN	225	0.006	SE	0.24
LAND.L	REA	232	0.006	GB	0.095
CFR.SW	TEX	228	0.01	CH	0.395
SSE.L	ELC	229	0.007	GB	0.19
GLE.PA	INS	241	0.006	FR	0.284
STERV.HE	FRP	249	0.008	FI	0.086
SY1.DE	CHM	218	0.006	DE	0.137
TUI1.DE	TRT	236	0.006	DE	0.072
UPM.HE	FRP	222	0.008	FI	0.178
VNA.DE	REA	222	0.006	DE	0.282
ZURN.SW	INS	233	0.006	CH	0.595

Notes: The twenty firms with the highest betweenness centrality, considering absolute values. The number of edges is representing the average number of edges during the whole period 2016-2020. *Source:* S&P Global and author's calculations.

Table A.11: *Average positive eigenvector centrality (C_E^+), 2016-2020*

Ticker	Industry	Num. Edges	C_E^+	ISO Code	Market Cap. %
STERV.HE	FRP	126	0.012	FI	0.086
CABK.MC	BNK	113	0.011	ES	0.181
BBVA.MC	BNK	114	0.01	ES	0.359
SSE.L	ELC	118	0.01	GB	0.19
CFR.SW	TEX	116	0.01	CH	0.395
LAND.L	REA	118	0.009	GB	0.095
BAS.DE	CHM	105	0.009	DE	0.669
CSGN.SW	FBN	105	0.009	CH	0.333
INVE-B.ST	FBN	119	0.009	SE	0.24
ALV.DE	INS	122	0.008	DE	0.985
HNR1.DE	INS	114	0.008	DE	0.225
UPM.HE	FRP	109	0.008	FI	0.178
OR.PA	COS	112	0.007	FR	1.59
LGEN.L	BNK	109	0.007	GB	0.229
LLOY.L	BNK	111	0.007	GB	0.561
NG.L	MUW	116	0.007	GB	0.453
SBRY.L	FDR	116	0.007	GB	0.065
EZJ.L	AIR	121	0.007	GB	0.072
GLE.PA	INS	127	0.007	FR	0.284
BARC.L	BNK	121	0.007	GB	0.393

Notes: The twenty firms with the highest betweenness centrality, considering positive values. The number of edges is representing the average number of edges during the whole period 2016-2020. *Source:* S&P Global and author's calculations.

Table A.12: *Average degree centralities, analysis by industry, 2016-202. Part I*

Industry	Market Cap %	Num. Firms	C_E^{abs}	C_E^{+}	C_D^{net}	C_D^{abs}	C_D^{+}	C_C^{abs}	C_C^{+}	C_H^{abs}	C_H^{+}	C_B^{abs}	C_B^{+}
DRG	10.72	11	0.054	0.054	0.852	6.498	3.675	0.06	0.054	20.76	18.70	0.003	0.003
BNK	8.93	27	0.055	0.054	0.953	6.747	3.85	0.061	0.055	21.32	19.37	0.003	0.004
TEX	5.85	10	0.057	0.057	0.793	6.903	3.848	0.061	0.055	21.39	19.14	0.003	0.004
OGX	5.76	9	0.054	0.054	0.922	6.62	3.771	0.06	0.054	21.06	18.93	0.003	0.004
INS	5.53	19	0.055	0.055	0.925	6.793	3.859	0.061	0.055	21.32	19.26	0.004	0.004
FOA	4.51	8	0.057	0.058	0.872	6.553	3.713	0.059	0.053	20.38	18.39	0.002	0.002
BVG	3.6	5	0.057	0.057	0.968	7.166	4.067	0.062	0.056	21.74	19.57	0.004	0.004
TLS	3.57	14	0.054	0.055	0.948	6.363	3.656	0.059	0.053	20.52	18.48	0.002	0.003
FBN	2.92	16	0.053	0.054	1.095	6.367	3.731	0.06	0.054	20.94	19.05	0.003	0.004
AUT	2.85	9	0.051	0.051	0.932	6.137	3.534	0.059	0.053	20.64	18.61	0.002	0.003
CHM	2.81	15	0.053	0.053	0.849	6.213	3.531	0.059	0.053	20.54	18.58	0.003	0.003
ELC	2.77	9	0.055	0.054	1.032	6.631	3.832	0.061	0.055	21.11	19.09	0.003	0.004
COS	2.74	3	0.055	0.056	1.111	6.719	3.915	0.061	0.055	21.27	19.33	0.003	0.005
ARO	2.54	7	0.057	0.057	0.856	6.564	3.71	0.06	0.054	20.74	18.66	0.002	0.003

Notes: The first twelve industries represent the 59.81% of participation in terms of market capitalization and in number of firms per industry. *Source:* S&P Global and author's calculations.

Table A.13: *Average degree centralities, analysis by industry, 2016-202. Part II*

Industry	Market Cap %	Num. Firms	C_E^{abs}	C_E^+	C_D^{net}	C_D^{abs}	C_D^+	C_C^{abs}	C_C^+	C_H^{abs}	C_H^+	C_B^{abs}	C_B^+
SOF	2.24	4	0.051	0.05	0.643	6.244	3.443	0.06	0.053	20.72	18.41	0.002	0.003
MNX	2.11	5	0.056	0.052	0.915	6.951	3.933	0.062	0.056	21.67	19.7	0.004	0.005
IEQ	2.03	14	0.055	0.055	0.781	6.494	3.638	0.06	0.053	20.80	18.57	0.002	0.003
PRO	1.96	11	0.054	0.055	0.914	6.18	3.547	0.058	0.052	20.15	18.21	0.002	0.002
MUW	1.74	9	0.052	0.05	0.77	6.428	3.599	0.06	0.054	21.17	19.13	0.003	0.004
SEM	1.72	3	0.057	0.054	1.089	7.032	4.061	0.062	0.057	21.98	20.23	0.004	0.005
RTS	1.58	4	0.055	0.055	0.678	6.404	3.541	0.059	0.053	20.61	18.47	0.002	0.003
REA	1.57	11	0.055	0.054	1.051	6.844	3.948	0.062	0.056	21.65	19.61	0.004	0.005
TRA	1.51	6	0.057	0.057	0.72	6.819	3.77	0.06	0.053	20.83	18.51	0.002	0.003
ELQ	1.44	5	0.055	0.058	0.902	6.696	3.799	0.06	0.054	20.90	18.60	0.003	0.003
TOB	1.34	3	0.058	0.055	0.787	7.257	4.022	0.062	0.056	21.75	19.78	0.004	0.005
CON	1.33	6	0.059	0.059	0.836	6.979	3.907	0.061	0.055	21.20	19.13	0.003	0.004
IDD	1.32	4	0.053	0.054	0.838	6.555	3.696	0.06	0.054	20.94	18.78	0.003	0.003
PUB	0.95	7	0.054	0.054	0.901	6.355	3.628	0.06	0.054	20.74	18.86	0.003	0.003

Notes: Twenty nine industries participate with 0.927% or less (per industry) of market capitalization, representing in total 12.04% of the index total.

Source: S&P Global and author's calculations.

Table A.14: *Average degree centralities, analysis by industry, 2016-202. Part III*

Industry	Market Cap %	Num. Firms	C_E^{abs}	C_E^{+}	C_D^{net}	C_D^{abs}	C_D^{+}	C_C^{abs}	C_C^{+}	C_H^{abs}	C_H^{+}	C_B^{abs}	C_B^{+}
MTC	0.93	4	0.052	0.053	0.968	6.394	3.681	0.06	0.054	20.98	18.90	0.003	0.004
FDR	0.91	6	0.055	0.055	1.054	6.597	3.826	0.06	0.055	21.03	19.17	0.003	0.004
COM	0.77	3	0.06	0.055	0.815	7.208	4.012	0.062	0.057	21.71	19.87	0.004	0.005
BLD	0.76	4	0.061	0.061	0.785	7.233	4.009	0.061	0.054	21.12	18.88	0.002	0.003
HOU	0.76	2	0.06	0.06	0.696	7.061	3.879	0.06	0.054	20.71	18.60	0.002	0.002
TSV	0.75	4	0.05	0.054	0.879	5.809	3.344	0.057	0.051	19.85	17.65	0.001	0.002
TCD	0.58	5	0.051	0.053	1.032	5.999	3.516	0.059	0.053	20.37	18.51	0.002	0.003
REX	0.55	2	0.061	0.06	0.731	7.278	4.005	0.061	0.054	21.41	18.91	0.003	0.004
ATX	0.54	3	0.054	0.054	0.725	6.333	3.529	0.059	0.053	20.45	18.38	0.002	0.003
TRT	0.51	5	0.056	0.056	0.829	6.79	3.809	0.06	0.054	21.04	18.82	0.003	0.003
AIR	0.49	4	0.05	0.049	0.761	6.167	3.464	0.06	0.053	21.02	18.75	0.003	0.004
GAS	0.47	3	0.052	0.05	0.899	6.307	3.603	0.061	0.055	21.34	19.19	0.003	0.004
CMT	0.46	2	0.052	0.05	0.558	5.887	3.222	0.058	0.051	20.05	18.00	0.002	0.003
HEA	0.46	2	0.05	0.051	0.838	6.16	3.499	0.06	0.054	20.65	18.64	0.002	0.003

Source: S&P Global and author's calculations.

Table A.15: *Average degree centralities, analysis by industry, 2016-202. Part IV*

Industry	Market Cap %	Num. Firms	C_E^{abs}	C_E^{+}	C_D^{net}	C_D^{abs}	C_D^{+}	C_C^{abs}	C_C^{+}	C_H^{abs}	C_H^{+}	C_B^{abs}	C_B^{+}
LIF	0.44	3	0.05	0.05	0.375	5.878	3.126	0.058	0.051	20.16	17.71	0.002	0.002
FRP	0.44	4	0.055	0.055	1.097	6.85	3.974	0.062	0.056	21.72	19.85	0.005	0.006
BTC	0.42	3	0.056	0.057	0.723	6.676	3.7	0.059	0.053	20.52	18.26	0.002	0.002
ITC	0.29	2	0.048	0.05	0.927	5.491	3.209	0.058	0.052	20.16	18.20	0.002	0.002
HOM	0.29	3	0.051	0.05	1.146	6.531	3.839	0.061	0.056	21.64	19.76	0.004	0.004
OGR	0.26	1	0.056	0.057	0.595	6.469	3.532	0.059	0.052	20.54	18.12	0.002	0.001
ICS	0.21	3	0.047	0.049	1.063	5.731	3.397	0.059	0.054	20.48	18.65	0.002	0.003
STL	0.17	1	0.047	0.05	1.194	5.731	3.463	0.059	0.053	20.50	18.52	0.002	0.003
CNO	0.16	2	0.056	0.055	0.894	6.532	3.713	0.06	0.054	21.04	18.96	0.003	0.003
CTR	0.16	2	0.058	0.056	0.831	6.882	3.856	0.061	0.055	21.18	19.14	0.003	0.004
THQ	0.08	1	0.059	0.064	1.273	6.867	4.07	0.059	0.053	20.46	18.25	0.002	0.002
IMS	0.07	1	0.049	0.05	0.458	5.603	3.031	0.057	0.05	19.71	17.31	0.001	0.001
ALU	0.07	1	0.057	0.054	0.505	6.97	3.738	0.062	0.056	21.44	19.57	0.003	0.004
DHP	0.07	1	0.046	0.045	0.15	4.96	2.555	0.055	0.048	19.01	16.43	0.001	0.001

Source: S&P Global and author's calculations.

Table A.16: *Average degree centralities, analysis by country, 2016-202*

Industry	Market Cap %	Num. Firms	C_E^{abs}	C_E^+	C_D^{net}	C_D^{abs}	C_D^+	C_C^{abs}	C_C^+	C_H^{abs}	C_H^+	C_B^{abs}	C_B^+
GB	22.7	84	0.054	0.054	0.931	6.529	3.73	0.06	0.054	21.00	18.99	0.003	0.004
FR	21.09	51	0.056	0.056	0.92	6.626	3.773	0.06	0.054	20.95	18.88	0.003	0.003
CH	13.72	30	0.054	0.054	0.907	6.574	3.74	0.061	0.054	21.08	18.97	0.003	0.004
DE	13.28	41	0.054	0.053	0.893	6.474	3.683	0.06	0.054	20.96	18.92	0.003	0.004
ES	5.49	18	0.057	0.057	1.022	6.932	3.977	0.061	0.055	21.34	19.33	0.003	0.004
NL	5.07	14	0.055	0.056	0.946	6.585	3.765	0.06	0.054	20.96	18.97	0.003	0.003
IT	4.52	19	0.053	0.052	0.768	6.227	3.497	0.059	0.053	20.65	18.52	0.002	0.003
SE	3.6	23	0.054	0.054	0.876	6.478	3.677	0.06	0.054	20.84	18.81	0.003	0.004
DK	2.57	11	0.052	0.052	0.798	6.024	3.411	0.058	0.052	20.22	18.22	0.002	0.002
BE	2.52	9	0.056	0.057	0.85	6.849	3.849	0.06	0.054	21.00	18.92	0.003	0.004
FI	1.92	10	0.056	0.056	0.88	6.852	3.866	0.061	0.055	21.32	19.14	0.004	0.004
NO	1.59	7	0.054	0.054	0.824	6.531	3.678	0.06	0.054	20.87	18.81	0.003	0.003
IE	1.12	8	0.056	0.054	0.573	6.548	3.56	0.06	0.053	20.77	18.62	0.002	0.003
AT	0.33	2	0.055	0.055	0.532	6.754	3.643	0.06	0.053	20.97	18.57	0.003	0.003
PT	0.25	2	0.057	0.059	1.146	6.515	3.831	0.059	0.053	20.48	18.51	0.002	0.002
LU	0.22	2	0.051	0.05	0.72	6.093	3.407	0.059	0.053	20.63	18.59	0.002	0.003

Notes: The first four countries represent the 70.7% and 62.2% of participation in terms of market capitalization and number of firms per industry respectively. *Source:* S&P Global and author's calculations.

Table A.17: *Network Description by Country*

			Normalized Weight				Normalized Number of Edges			
ISO	Number	Market		COVID-19				COVID-19		
code	of firms	Cap. %	Sans	Pre	During	Post	Sans	Pre	During	Post
GB	84	22.7	0.009	0.009	0.009	0.009	0.261	0.26	0.261	0.262
FR	51	21.09	0.011	0.01	0.01	0.011	0.283	0.285	0.29	0.283
CH	30	13.72	0.022	0.023	0.023	0.023	0.326	0.325	0.325	0.328
DE	41	13.28	0.014	0.014	0.014	0.014	0.274	0.271	0.272	0.28
ES	18	5.49	0.033	0.033	0.033	0.033	0.388	0.4	0.386	0.371
NL	14	05.07	0.017	0.017	0.017	0.018	0.288	0.301	0.313	0.316
IT	19	4.52	0.036	0.036	0.037	0.037	0.407	0.406	0.407	0.413
SE	23	3.61	0.025	0.025	0.025	0.026	0.351	0.357	0.352	0.34
DK	11	2.57	0.044	0.042	0.042	0.043	0.51	0.505	0.484	0.486
BE	9	2.52	0.035	0.036	0.035	0.035	0.419	0.439	0.414	0.396
FI	10	1.92	0.049	0.048	0.048	0.047	0.427	0.429	0.431	0.375
NO	7	1.59	0.073	0.073	0.075	0.075	0.578	0.597	0.652	0.614
IE	8	1.12	0.017	0.016	0.017	0.016	0.224	0.206	0.233	0.215
AT	2	0.33	0.149	0.139	0.149	0.161	1.0	1.0	1.0	1.0
PT	2	0.25	0.108	0.105	0.096	0.123	1.0	1.0	1.0	1.0
LU	2	0.22	0.0	0.0	0.0	0.0	0.0	0.0	0.0	0.0

Notes: This table shows the country with its corresponding market capitalization share from the most representative share to the smallest. The country is represented by its ISO code, followed by the number of firms per sector; it also shows the normalized weight of the edges among the sector and the normalized number of edges, considering net values. *Source:* S&P Global and author's calculations.

Table A.18: *Normalized Number of Edges per Industry*

	Firm	Total	Sans	Pre	Dur	Post
BNK	27	0.344	0.344	0.340	0.351	0.343
INS	19	0.386	0.385	0.384	0.398	0.392
FBN	16	0.359	0.359	0.358	0.360	0.360
CHM	15	0.365	0.364	0.387	0.355	0.354
IEQ	14	0.392	0.391	0.386	0.412	0.396
TLS	14	0.474	0.474	0.481	0.464	0.486
REA	11	0.501	0.503	0.484	0.503	0.486
PRO	11	0.342	0.340	0.349	0.360	0.346
DRG	11	0.450	0.452	0.427	0.455	0.444
TEX	10	0.448	0.449	0.440	0.440	0.454
AUT	9	0.495	0.497	0.501	0.479	0.467
ELC	9	0.493	0.497	0.473	0.480	0.460
OGX	9	0.722	0.728	0.700	0.699	0.677
MUW	9	0.432	0.432	0.410	0.424	0.463
FOA	8	0.348	0.343	0.386	0.331	0.391
PUB	7	0.580	0.578	0.589	0.588	0.585
ARO	7	0.641	0.64	0.658	0.659	0.598
FDR	6	0.641	0.643	0.645	0.603	0.650
CON	6	0.412	0.415	0.379	0.392	0.433
TRA	6	0.604	0.603	0.583	0.652	0.572
ELQ	5	0.543	0.545	0.476	0.582	0.538
TRT	5	0.794	0.793	0.800	0.800	0.800
TCD	5	0.639	0.648	0.63	0.600	0.533
BVG	5	0.704	0.705	0.693	0.699	0.700
MNX	5	0.873	0.874	0.839	0.887	0.900
TSV	4	0.391	0.406	0.264	0.339	0.397
BLD	4	0.374	0.378	0.383	0.345	0.337
FRP	4	0.837	0.825	0.865	0.875	0.962
AIR	4	1.0	1.0	1.0	1.0	1.0
MTC	4	0.790	0.784	0.819	0.833	0.785
RTS	4	0.388	0.382	0.383	0.433	0.446
IDD	4	0.390	0.390	0.383	0.363	0.452
SOF	4	0.838	0.842	0.833	0.833	0.785

Notes: Industries with more than 3 firms. *Source:* Author's calculations.

From Section 5.3

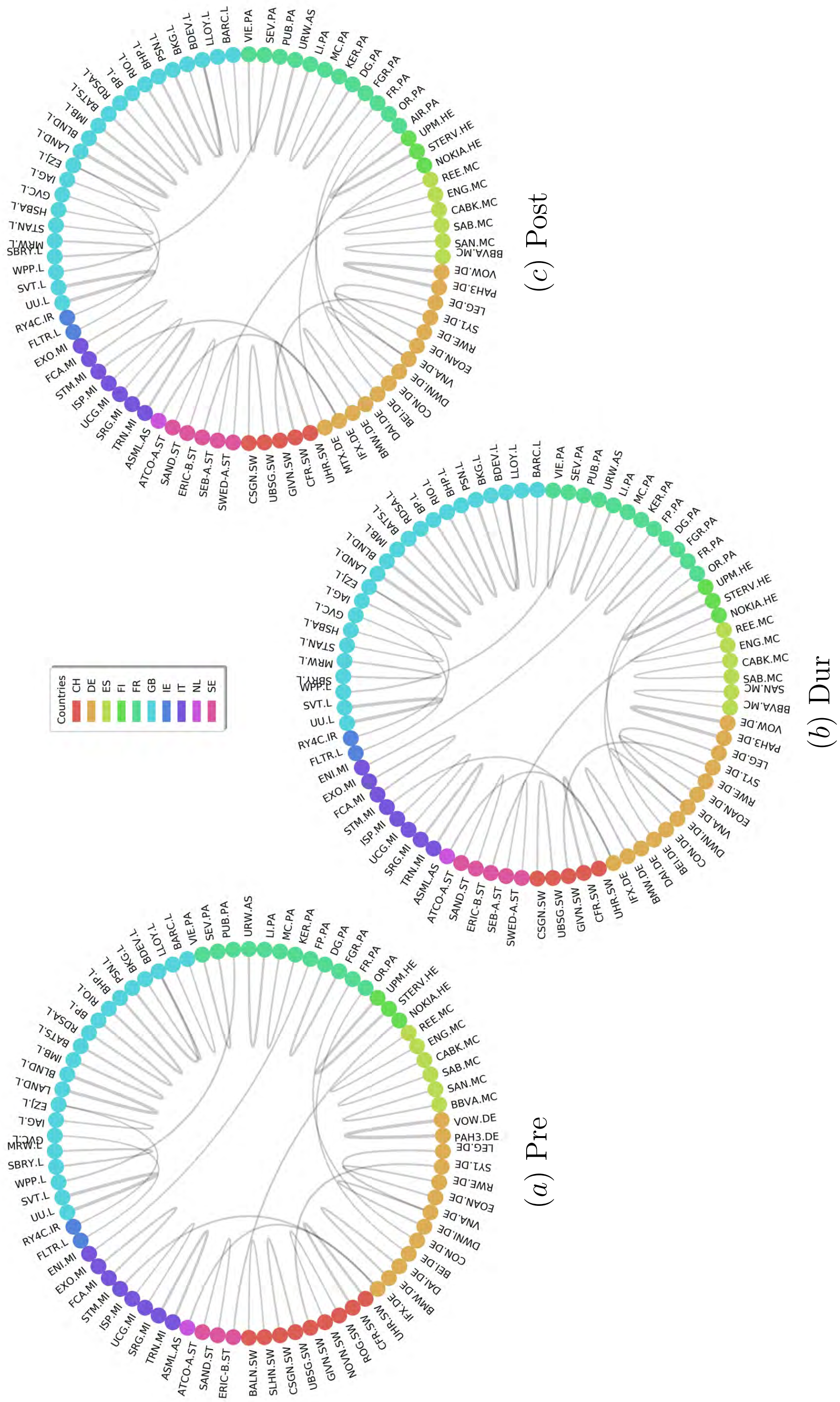

(a) Pre

(b) Dur

(c) Post

Figure A.5: Net (and absolute) partial correlation networks coloured by country. Only edges whose weight is greater or equal than 0.3 are considered in this picture. *Source:* Author's calculations.

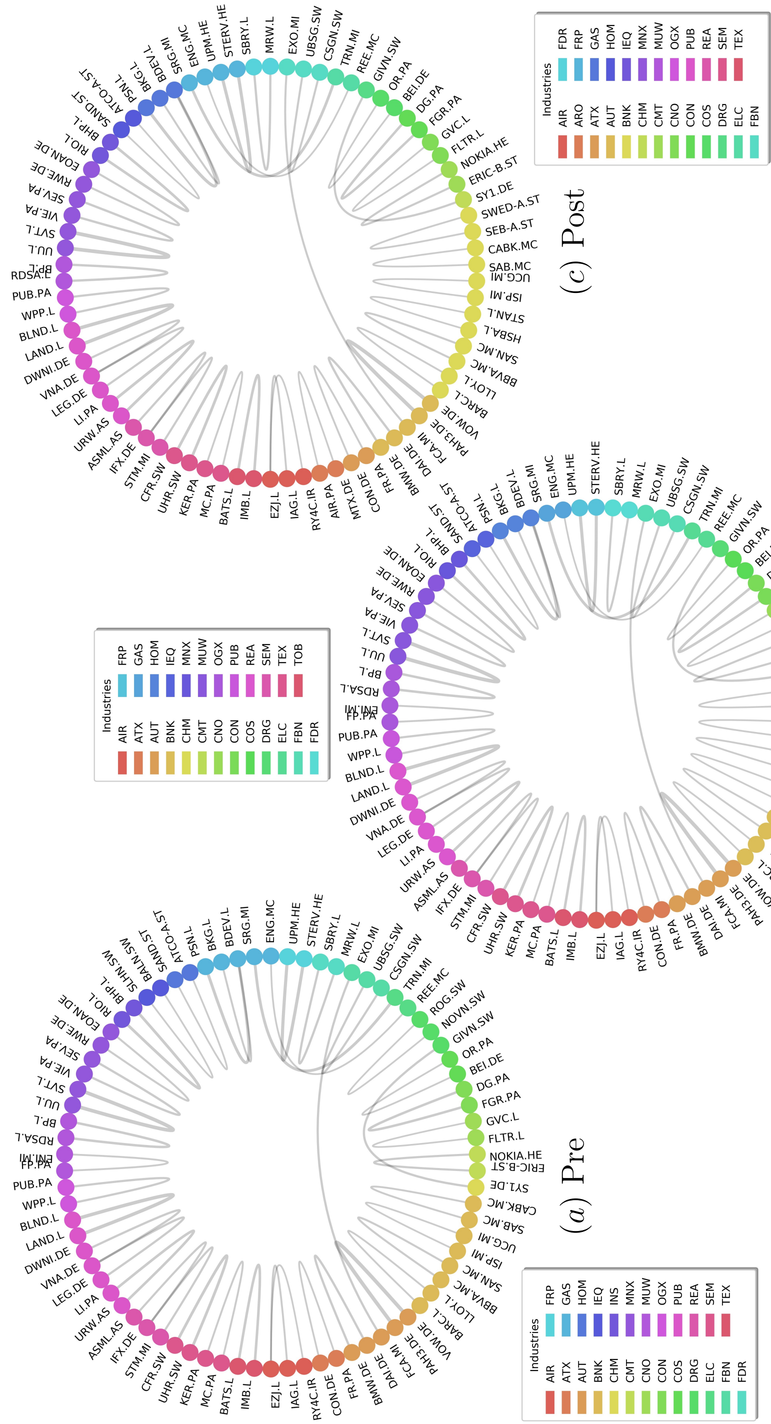

Figure A.6: Net (and absolute) partial correlation networks coloured by sector. Only edges whose weight is greater or equal than 0.3 are considered in this picture. *Source:* Author's calculations.

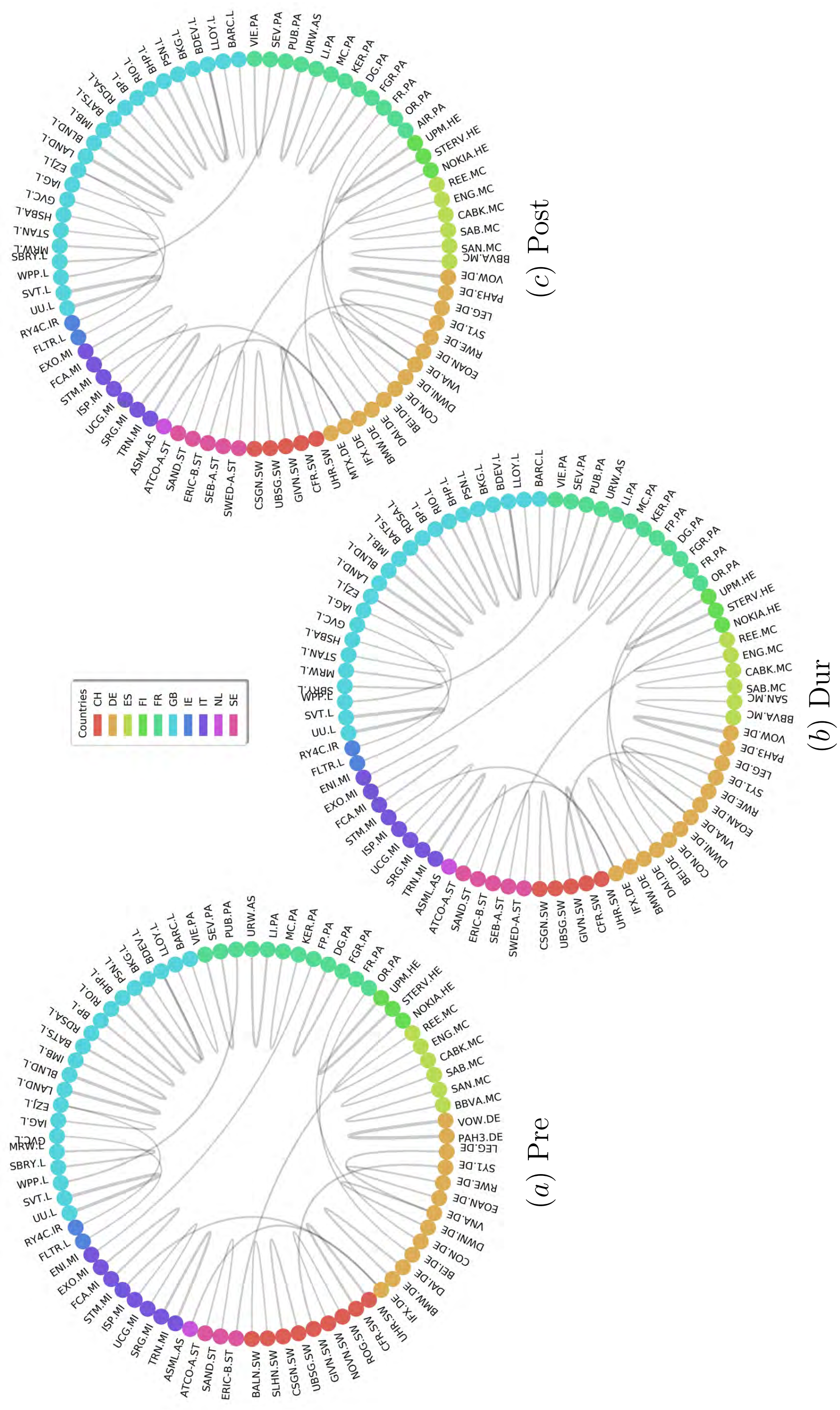

(a) Pre

(b) Dur

(c) Post

Figure A.7: Positive partial correlation networks coloured by country. Only edges whose weight is greater or equal than 0.3 are considered in this picture. *Source:* Author's calculations.

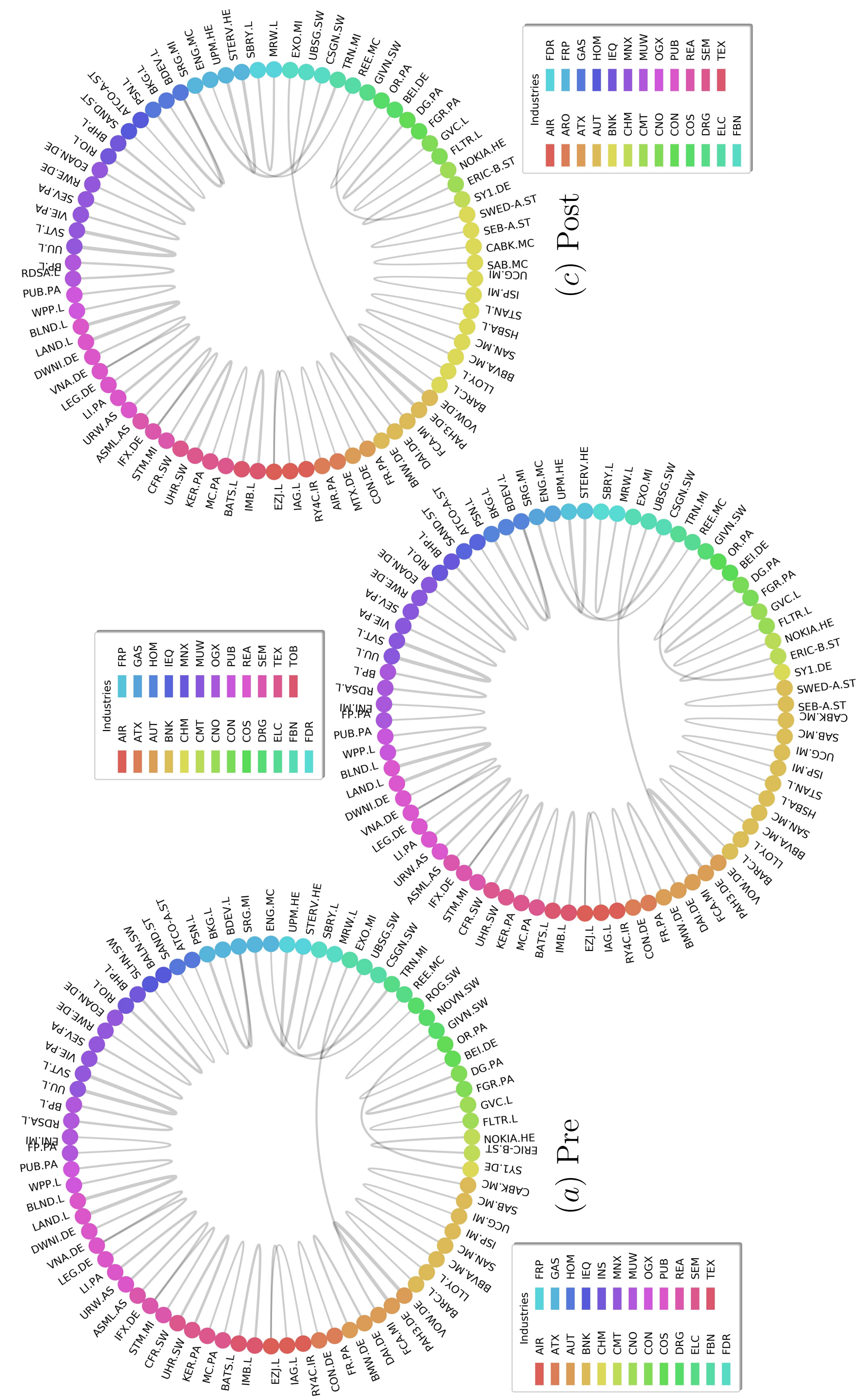

(*a*) Pre

(*b*) Dur

(*c*) Post

Figure A.8: Positive partial correlation networks coloured by sector. Only edges whose weight is greater or equal than 0.3 are considered in this picture. *Source:* Author's calculations.

From Section 5.4

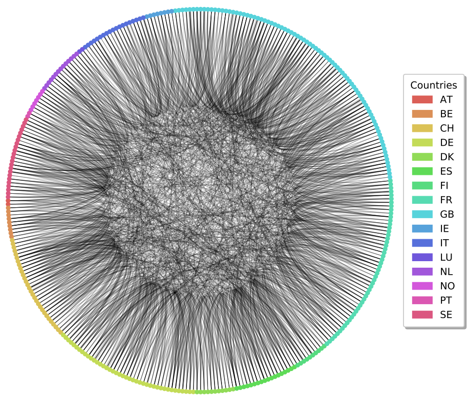

(a) $k = 0.058$, $h = 0.199$

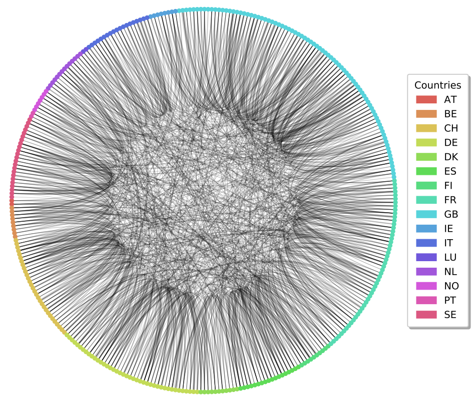

(b) $k = 0.1$, $h = 0.227$

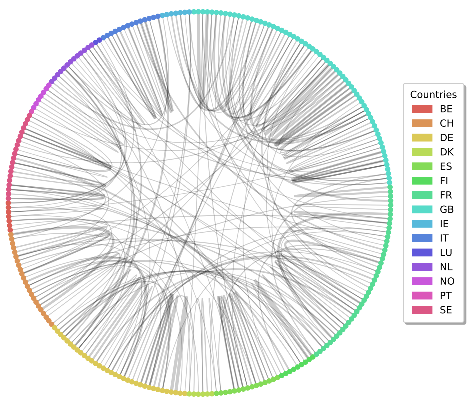

(c) $k = 0.15$, $h = 0.488$

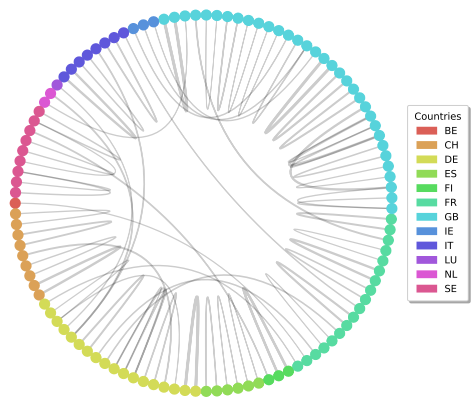

(d) $k = 0.25$, $h = 0.758$

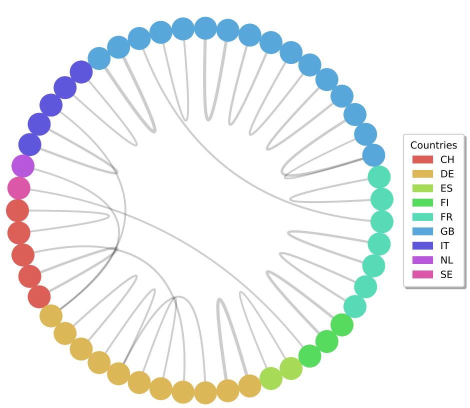

(e) $k = 0.35$, $h = 0.815$

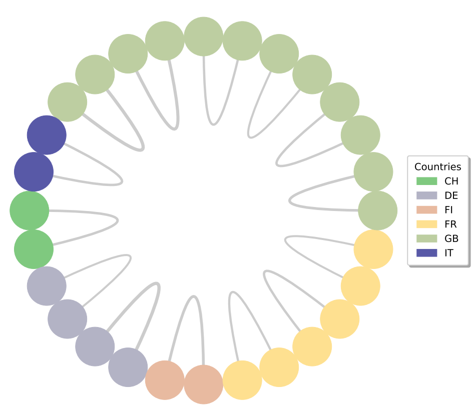

(f) $k = 0.4$, $h = 1$

Figure A.9: Homophily by country in the net skeleton, each subfigure was drawn using a diffferent cut-off value k, obtaining the homophily ratio h. *Source:* Author's calculations.

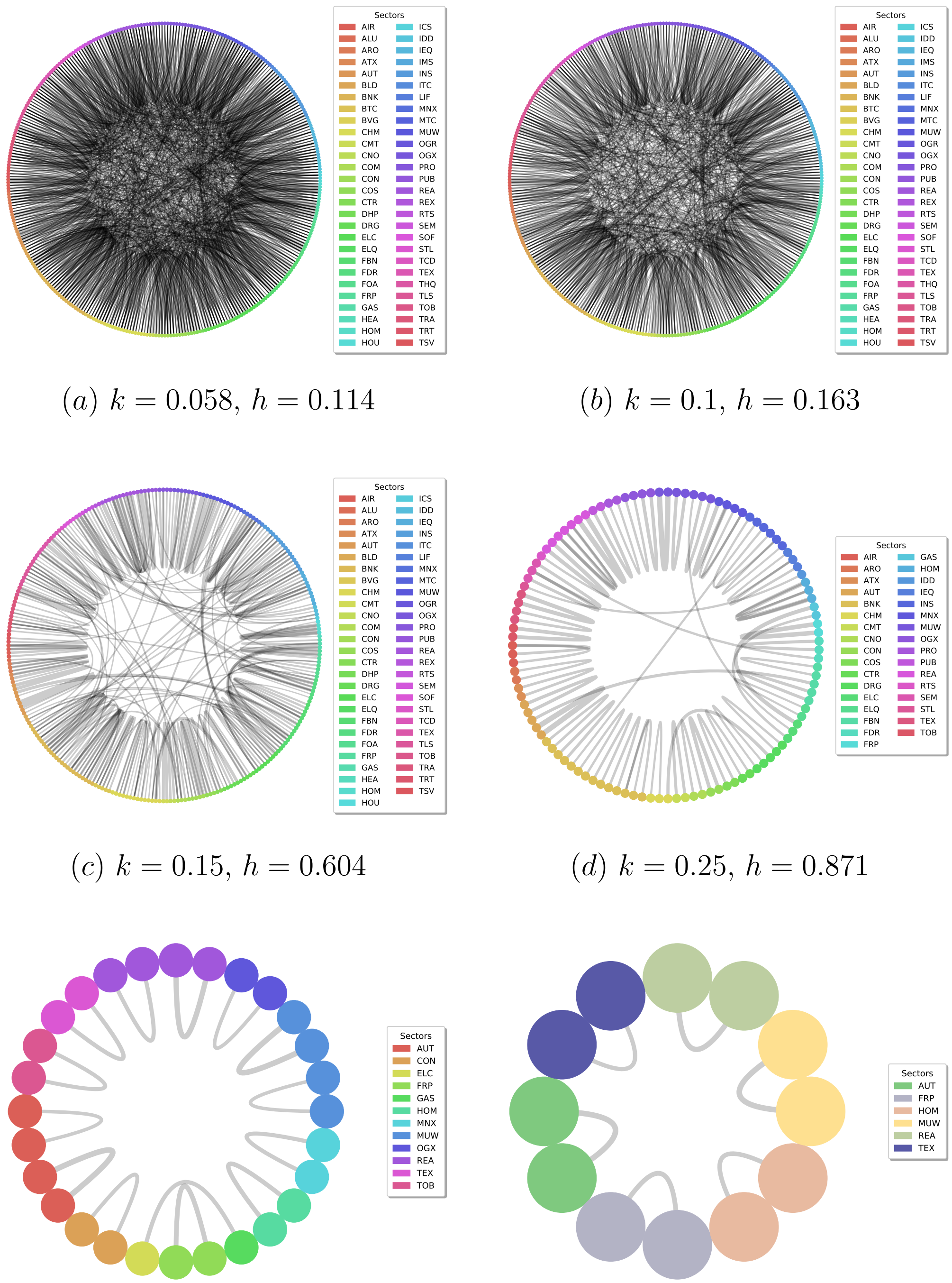

(a) $k = 0.058$, $h = 0.114$ (b) $k = 0.1$, $h = 0.163$

(c) $k = 0.15$, $h = 0.604$ (d) $k = 0.25$, $h = 0.871$

(e) $k = 0.4$, $h = 0.929$ (f) $k = 0.5$, $h = 1$

Figure A.10: Homophily by sector in the net skeleton, each subfigure was drawn using a diffferent cut-off value k, obtaining the homophily ratio h. *Source:* Author's calculations.

A.2.1 Tickers, Countries and Industries

Table A.19: *Firms Part I*

Ticker	Firm	Market Cap	ISO Code	Industry Code
1COV.DE	Covestro AG	7585 350000	DE	CHM
AAL.L	Anglo American PLC	35532 325635	GB	MNX
ABBN.SW	ABB Ltd	46631 121398	CH	ELQ
ABF.L	Associated British Foods	24306 770982	GB	FOA
ABI.BR	Anheuser Busch Inbev NV	123000 000000	BE	BVG
ABN.AS	ABN AMRO Group NV	15246 800000	NL	BNK
AC.PA	Accor	11274 420500	FR	TRT
ACA.PA	Credit Agricole SA	37284 605325	FR	BNK
ACS.MC	ACS Actividades de Construccion y Servicios SA	11217 807250	ES	CON
AD.AS	Ahold Delhaize NV	26391 148875	NL	FDR
ADP.PA	ADP Promesses	17427 032100	FR	PRO
ADS.DE	Adidas AG	58080 556800	DE	TEX
AENA.MC	Aena SA	25575 000000	ES	TRA
AGN.AS	Aegon NV	8523 000416	NL	INS
AGS.BR	AGEAS	10450 342320	BE	INS
AHT.L	Ashtead Group	14359 138055	GB	TCD
AI.PA	L'Air Liquide S.A.	59445 121800	FR	CHM
AIR.PA	Airbus SE	101000 000000	FR	ARO
AKE.PA	Arkema	7242 750700	FR	CHM
AKZA.AS	Akzo Nobel NV	20643 260000	NL	CHM
ALFA.ST	Alfa Laval AB	9490 388121	SE	IEQ
ALO.PA	Alstom	9472 357920	FR	IEQ
ALV.DE	Allianz SE	91110 583200	DE	INS
AMS.MC	Amadeus IT Group SA	31396 310400	ES	TSV
ASML.AS	ASML Holding NV	112000 000000	NL	SEM
ASSA-B.ST	Assa Abloy B	22025 237708	SE	BLD
ATCO-A.ST	Atlas Copco AB A	29893 459353	SE	IEQ
ATL.MI	Atlantia SpA	17153 267670	IT	TRA
ATO.PA	AtoS SE	8115 372400	FR	TSV
AV.L	Aviva	19478 435620	GB	INS
AZN.L	AstraZeneca PLC	118000 000000	GB	DRG

Source: S&P Global and author.

Table A.20: *Firms Part II*

Ticker	Firm	Market Cap	ISO Code	Industry Code
BA.L	BAE Systems PLC	23152 520936	GB	ARO
BAER.SW	Julius Baer Group	10284 124741	CH	FBN
BALN.SW	Baloise Hldg Reg	7859 340301	CH	INS
BARC.L	Barclays	36376 018151	GB	BNK
BAS.DE	BASF SE	61859 560650	DE	CHM
BATS.L	British American Tobacco PLC	94014 870214	GB	TOB
BAYN.DE	Bayer AG	67899 111120	DE	DRG
BBVA.MC	Banco Bilbao Vizcaya Argentaria SA	33226 080921	ES	BNK
BDEV.L	Barratt Developments	8981 456822	GB	HOM
BEI.DE	Beiersdorf AG	26875 800000	DE	COS
BHP.L	BHP Group Plc	44349 528279	GB	MNX
BIRG.IR	Bank of Ireland Group	5270 162938	IE	BNK
BKG.L	Berkeley Group Holdings Plc	7860 684449	GB	HOM
BLND.L	British Land Co	7108 239101	GB	REA
BMW.DE	Bayer Motoren Werke AG (BMW)	44029 914300	DE	AUT
BN.PA	danone	50625 564500	FR	FOA
BNP.PA	BNP Paribas	65744 980290	FR	BNK
BNR.DE	Brenntag AG	7490 160000	DE	TCD
BNZL.L	Bunzl	8190 216743	GB	TCD
BOL.ST	Boliden AB	6478 950144	SE	MNX
BP.L	BP p.l.c	120000 000000	GB	OGX
BRBY.L	Burberry Group	10719 812115	GB	TEX
BT-A.L	BT Group	22669 956904	GB	TLS
BVI.PA	Bureau Veritas SA	10512 101140	FR	PRO
CA.PA	Carrefour SA	12068 626700	FR	FDR
CABK.MC	CaixaBank	16736 063524	ES	BNK
CAP.PA	Capgemini SE	18218 316600	FR	TSV
CARL-B.CO	Carlsberg AS B	15807 271025	DK	BVG
CBK.DE	Commerzbank AG	6909 259086	DE	BNK
CCL.L	Carnival Plc	9321 627486	GB	TRT
CFR.SW	Richemont, Cie Financiere A Br	36538 864514	CH	TEX
CHR.CO	Christian Hansen Holding A/S	9341 145735	DK	LIF
CLN.SW	Clariant AG Reg	6598 424555	CH	CHM

Source: S&P Global and author.

Table A.21: *Firms Part III*

Ticker	Firm	Market Cap	ISO Code	Industry Code
CLNX.MC	Cellnex Telecom S.A.	14784 996990	ES	TLS
CNA.L	Centrica	6152 218228	GB	MUW
CNHI.MI	CNH Industrial NV	13325 257110	IT	IEQ
COLO-B.CO	Coloplast AS B	21897 018624	DK	HEA
CON.DE	Continental AG	23052 691560	DE	ATX
CPG.L	Compass Group	35582 324369	GB	REX
CRDA.L	Croda Intl	7981 408595	GB	CHM
CRH	CRH Plc	28198 133760	IE	COM
CS.PA	AXA	60928 360380	FR	INS
CSGN.SW	Credit Suisse Group AG	30826 778129	CH	FBN
DAI.DE	Daimler AG	52817 852690	DE	AUT
DANSKE.CO	Danske Bank A/S	12437 947310	DK	BNK
DASTY	Dassault Systemes SA	38532 098400	FR	SOF
DB	Deutsche Bank AG	14295 868841	DE	BNK
DB1.DE	Deutsche Boerse AG	26628 500000	DE	FBN
DCC.L	DCC	7836 826228	IE	IDD
DG.PA	Vinci	59918 562000	FR	CON
DGE.L	Diageo Plc	97310 307888	GB	BVG
DLG.L	Direct Line Insurance Group	5078 020620	GB	INS
DNB.OL	DNB ASA	26283 427706	NO	BNK
DPW.DE	Deutsche Post AG	41805 942250	DE	TRA
DSM.AS	Koninklijke DSM NV	21063 442500	NL	CHM
DSV.CO	Dsv Panalpina A/s	24146 014608	DK	TRA
DTE.DE	Deutsche Telekom AG	69374 457630	DE	TLS
DWNI.DE	Deutsche Wohnen AG BR	13100 456100	DE	REA
EBS.VI	Erste Group Bank AG	14424 088000	AT	BNK
EDEN.PA	Edenred	11211 750500	FR	TSV
EDF.PA	Electricite de France	30290 030160	FR	ELC
EDP.LS	Energias de Portugal SA	11931 027360	PT	ELC
EL.PA	EssilorLuxottica	58853 004000	FR	TEX
ELE.MC	Endesa SA	25187 710080	ES	ELC
ELISA.HE	Elisa Corporation	8190 669000	FI	TLS
ELUX-B.ST	Electrolux AB B	6571 380437	SE	DHP
EN.PA	Bouygues	14072 723040	FR	CON
ENEL.MI	Enel SpA	71827 885376	IT	ELC
ENG.MC	Enagas SA	5428 811160	ES	GAS
ENGI.PA	Engie	34731 072000	FR	MUW

Source: S&P Global and author.

Table A.22: *Firms Part IV*

Ticker	Firm	Market Cap	ISO Code	Industry Code
ENI.MI	ENI SpA	50318 925510	IT	OGX
EOAN.DE	E.ON SE	25155 922156	DE	MUW
EQNR.OL	Equinor ASA	59422 071034	NO	OGX
ERIC-B.ST	Ericsson L.M. Telefonaktie B	23660 551313	SE	CMT
EXO.MI	EXOR NV	16648 280000	IT	FBN
EXPN.L	Experian Plc	29221 182071	GB	PRO
EZJ.L	Easyjet	6659 805941	GB	AIR
FCA.MI	Fiat Chrysler Automobiles NV	20446 042518	IT	AUT
FER.MC	Ferrovial SA	19942 211340	ES	CON
FERG.L	Ferguson PLC	18780 339920	GB	TCD
FGR.PA	Eiffage	9996 000000	FR	CON
FLTR.L	Flutter Entertainment plc	8465 277150	IE	CNO
FME.DE	Fresenius Medical Care AG	20259 086320	DE	HEA
FORTUM.HE	Fortum Oyj	19544 074000	FI	ELC
FP.PA	TOTAL SA	131000 000000	FR	OGX
FR.PA	Valeo	7546 346730	FR	ATX
G.MI	Assicurazioni Generali SpA	28638 458095	IT	INS
G1A.DE	GEA AG	5320 904160	DE	IEQ
GALP.LS	Galp Energia SGPS SA	11490 447900	PT	OGX
GBLB.BR	Groupe Bruxelles Lambert	15161 197680	BE	FBN
GEBN.SW	Geberit AG Reg	18517 002581	CH	BLD
GFC.PA	Gecina	12155 614800	FR	REA
GFS.L	G4S Plc	3997 388193	GB	ICS
GIVN.SW	Givaudan AG	25757 519041	CH	DRG
GLE.PA	Societe Generale	26292 438995	FR	INS
GLEN.L	Glencore Plc	40569 355368	GB	MNX
GLPG.AS	Galapagos Genomics NV	12060 395500	BE	BTC
GMAB.CO	Genmab AS	12880 438320	DK	BTC
GRF.MC	Grifols SA	13393 265900	ES	BTC
GSK.L	GlaxoSmithKline	113000 000000	GB	DRG
GVC.L	GVC Holdings PLC	6041 813756	GB	CNO
HEI.DE	HeidelbergCement AG	12889 103360	DE	COM
HEIA.AS	Heineken NV	54674 204760	NL	BVG
HEN3.DE	Henkel AG & Co. KGaA Nvtg - Pref	16426 628600	DE	HOU
HEXA-B.ST	Hexagon AB	17520 937593	SE	ITC
HL.L	Hargreaves Lansdown Plc	10846 590177	GB	FBN
HLMA.L	Halma	9449 553980	GB	ITC

Source: S&P Global and author.

Table A.23: *Firms Part V*

Ticker	Firm	Market Cap	ISO Code	Industry Code
HM-B.ST	Hennes & Mauritz AB B	26521 955023	SE	RTS
HNR1.DE	Hannover Ruck SE	20778 863100	DE	INS
HO.PA	Thales	19586 946600	FR	ARO
HSBA.L	HSBC Holdings Plc	144000 000000	GB	BNK
IAG.L	International Consolidated Airlines Group SA	14713 577672	GB	AIR
IMB.L	Imperial Brands PLC	22548 389450	GB	TOB
IMI.L	IMI	3988 017359	GB	PRO
INDU-A.ST	Industrivarden AB A	5938 978289	SE	FBN
INF.L	Informa PLC	12676 181930	GB	PUB
INGA.AS	ING Groep NV	41645 321728	NL	BNK
IBE.MC	Iberdrola SA	58403 820960	ES	ELC
IFX.DE	Infineon Technologies AG	25391 338590	DE	SEM
IHG.L	InterContinental Hotels Group PLC	11553 634759	GB	TRT
III.L	3I Group	12602 800553	GB	FBN
INVE-B.ST	Investor AB B	22195 627041	SE	FBN
ISP.MI	Intesa SanPaolo	41114 341692	IT	BNK
ITRK.L	Intertek Group PLC	11119 592874	GB	PRO
ITV.L	ITV PLC	7183 377677	GB	PUB
ITX.MC	Inditex SA	98018 642500	ES	RTS
JMAT.L	Johnson, Matthey	7043 813456	GB	CHM
KBC.BR	KBC Group NV	27961 807020	BE	BNK
KER.PA	Kering	73803 668400	FR	TEX
KGP.L	Kingspan Group PLC	9888 392250	IE	BLD
KINV-B.ST	Kinnevik Investment AB B	5280 737098	SE	FBN
KNEBV.HE	Kone Corp B	26178 851480	FI	IEQ
KNIN.SW	KUEHNE & NAGEL INTL AG-REG	18023 105439	CH	TRA
KPN.AS	Koninklijke KPN NV	11057 682564	NL	TLS
KYGA.L	Kerry Group A	19531 935500	IE	FOA
LAND.L	Land Securities Group PLC	8789 760224	GB	REA
LDO.MI	Leonardo S.p.a.	6041 667500	IT	ARO
LEG.DE	LEG Immobilien AG	7237 880150	DE	REA
LGEN.L	Legal & General Group	21154 473153	GB	BNK
LHA.DE	Deutsche Lufthansa AG	7772 662140	DE	AIR
LHN.SW	LafargeHolcim Ltd	30439 194891	CH	COM
LI.PA	Klepierre	10406 302400	FR	REA

Source: S&P Global and author.

Table A.24: *Firms Part VI*

Ticker	Firm	Market Cap	ISO Code	Industry Code
LISN.SW	Lindt & Sprungli AG Reg	10701 218854	CH	FOA
LLOY.L	Lloyds Banking Group PLC	51831 247152	GB	BNK
LOGN.SW	Logitech International SA	7301 174195	CH	THQ
LONN.SW	Lonza AG	24206 078639	CH	LIF
LR.PA	Legrand Promesses	19234 418240	FR	ELQ
LSE.L	London Stock Exchange PLC	32084 185501	GB	FBN
LXS.DE	Lanxess AG	5231 139360	DE	CHM
MAERSK-A.CO	AP Moller - Maersk AS A	12997 745612	DK	TRA
MB.MI	Mediobanca SpA	8648 440290	IT	BNK
MC.PA	LVMH-Moet Vuitton	211000 000000	FR	TEX
MCRO.L	Micro Focus International	4561 232100	GB	PRO
MKS.L	Marks & Spencer Group	4920 181628	GB	FDR
ML.PA	Michelin CGDE B Brown	19645 200600	FR	ATX
MNDI.L	Mondi PLC	10171 043700	GB	FRP
MONC.MI	Moncler SpA	10336 016430	IT	TEX
MOWI.OL	Mowi ASA	11942 557638	NO	FOA
MRK.DE	MERCK KGaA	13615 644700	DE	DRG
MRO.L	Melrose Industries PLC	13785 236033	GB	IEQ
MRW.L	Morrison (WM) Supermarkets	5650 440187	GB	FDR
MT.AS	ArcelorMittal Inc	15888 392784	LU	STL
MTX.DE	MTU Aero Engines AG	13239 200000	DE	ARO
MUV2.DE	Munich Re AG	37955 634000	DE	INS
NDA-FI.HE	Nordea Bank Abp	29111 104460	FI	BNK
NESN.SW	Nestle SA Reg	287000 000000	CH	FOA
NESTE.HE	Neste Oyj	23860 956240	FI	OGR
NG.L	National Grid PLC	41881 362823	GB	MUW
NHY.OL	Norsk Hydro AS	6848 706583	NO	ALU
NN.AS	NN Group N.V.	11619 063920	NL	INS
NOKIA.HE	Nokia OYJ	18561 447072	FI	CMT
NOVN.SW	Novartis AG Reg	216000 000000	CH	DRG
NOVO-B.CO	Novo Nordisk AS B	96373 738885	DK	DRG
NTGY.MC	Naturgy Energy Group SA	22044 332800	ES	GAS
NXT.L	Next	11049 786129	GB	RTS
NZYM-B.CO	Novozymes AS B	10350 570630	DK	CHM
OCDO.L	Ocado Group PLC	10685 197490	GB	RTS

Source: S&P Global and author.

Table A.25: *Firms Part VII*

Ticker	Firm	Market Cap	ISO Code	Industry Code
OMV.VI	OMV AG	16389 831840	AT	OGX
OR.PA	L'Oreal	147000 000000	FR	COS
ORA.PA	Orange	34750 589760	FR	TLS
ORK.OL	Orkla AS	9034 708498	NO	FOA
PAH3.DE	Porsche Automobil Holding SE	10204 250000	DE	AUT
PGHN.SW	Partners Group Hldg	21805 141471	CH	REA
PHIA.AS	Koninklijke Philips Electronics NV	39397 568000	NL	MTC
PNDORA.CO	Pandora A/S	3878 179176	DK	TEX
PROX.BR	Proximus	8626 398000	BE	ELQ
PRU.L	Prudential PLC	44280 510043	GB	INS
PRY.MI	Prysmian SpA	5762 414560	IT	ELQ
PSN.L	Persimmon	10114 746939	GB	HOM
PSON.L	Pearson	5876 761866	GB	PUB
PUB.PA	Publicis Groupe	9701 292840	FR	PUB
QIA.DE	QIAGEN NV	6913 384360	DE	LIF
RACE.MI	Ferrari NV	28681 211700	IT	AUT
RAND.AS	Randstad NV	9960 451280	NL	PRO
RB.L	Reckitt Benckiser Group PLC	53348 811760	GB	HOU
RDSA.L	Royal Dutch Shell PLC	110000 000000	GB	OGX
REE.MC	Red Electrica Corporacion SA	9698 859000	ES	ELC
REL.L	RELX PLC	45300 422373	GB	PRO
REP.MC	Repsol SA	22271 158630	ES	OGX
RI.PA	Pernod-Ricard	42290 573400	FR	BVG
RIO.L	Rio Tinto PLC	67920 021937	GB	MNX
RMS.PA	Hermes Intl	70330 067800	FR	TEX
RNO.PA	Renault SA	12473 553960	FR	AUT
ROG.SW	Roche Hldgs AG Ptg Genus	203000 000000	CH	DRG
RR.L	Rolls-Royce Holdings PLC	15590 884245	GB	ARO
RSA.L	RSA Insurance Group PLC	6861 117604	GB	INS
RTO.L	Rentokil Initial	9836 210575	GB	ICS
RWE.DE	RWE AG	16813 303100	DE	MUW
RY4C.IR	Ryanair Holdings PLC	15859 007780	IE	AIR
SAB.MC	Banco de Sabadell SA	5840 797040	ES	BNK

Source: S&P Global and author.

Table A.26: *Firms Part VIII*

Ticker	Firm	Market Cap	ISO Code	Industry Code
SAF.PA	Safran SA	56314 955050	FR	ARO
SAMPO.HE	Sampo Oyj A	21562 054320	FI	INS
SAN.MC	Banco Santander SA	61985 568950	ES	BNK
SAN.PA	Sanofi-Aventis	113000 000000	FR	DRG
SAND.ST	Sandvik AB	21857 965979	SE	IEQ
SAP.DE	SAP SE	148000 000000	DE	SOF
SBRY.L	Sainsbury (J)	6008 030226	GB	FDR
SCA-B.ST	SCA - B shares	5774 424878	SE	FRP
SCHN.SW	Schindler-Hldg AG Reg	14642 544020	CH	IEQ
SCMN.SW	Swisscom AG Reg	24437 307425	CH	TLS
SCR.PA	SCOR SE	6980 326800	FR	INS
SDR.L	Schroders PLC	8905 494694	GB	FBN
SEB-A.ST	SEB-Skand Enskilda Banken A	18219 828720	SE	BNK
SECU-B.ST	Securitas AB B	5354 462712	SE	ICS
SESG.PA	SES	4793 225000	LU	PUB
SEV.PA	Suez SA	8406 050055	FR	MUW
SGE.L	Sage Group	9912 283546	GB	SOF
SGO.PA	Saint-Gobain, Cie de	19940 789500	FR	BLD
SGRO.L	SEGRO PLC	11627 787008	GB	REA
SGSN.SW	SGS-Soc Gen Surveil Hldg Reg	18624 735178	CH	PRO
SHB-A.ST	Svenska Handelsbanken A	18699 691239	SE	BNK
SIE.DE	Siemens AG	99059 000000	DE	IDD
SK3.IR	Smurfit Kappa Group PLC	8096 425980	IE	CTR
SKA-B.ST	SKANSKA AB-B	8072 421673	SE	CON
SKF-B.ST	SKF AB B	7588 180375	SE	IEQ
SLA.L	Standard Life Aberdeen	9100 512935	GB	FBN
SLHN.SW	Swiss Life Reg	15019 669587	CH	INS
SMDS.L	DS Smith	6209 762969	GB	CTR
SMIN.L	Smiths Group	7829 724427	GB	IDD
SN.L	Smith & Nephew	19295 676774	GB	MTC
SOLB.BR	Solvay	10936 990800	BE	CHM
SOON.SW	Sonova Holding AG	13127 267443	CH	MTC
SPSN.SW	Swiss Prime Site AG	7821 016722	CH	REA
SPX.L	Spirax-Sarco Engineering	7724 540020	GB	IEQ
SREN.SW	Swiss Re Reg	32752 395869	CH	INS
SRG.MI	Snam SpA	15908 224926	IT	GAS

Source: S&P Global and author.

Table A.27: *Firms Part IX*

Ticker	Firm	Market Cap	ISO Code	Industry Code
SSE.L	Scottish & Southern Energy	17583 650712	GB	ELC
STAN.L	Standard Chartered	26909 227396	GB	BNK
STERV.HE	Stora Enso OYJ R	7939 610420	FI	FRP
STJ.L	St James's Place	7280 987158	GB	FBN
STM.MI	STMicroelectronics NV	21820 346430	IT	SEM
STMN.SW	Straumann AG Reg	13888 578547	CH	MTC
SU.PA	Schneider Electric SE	53251 444500	FR	ELQ
SVT.L	Severn Trent	7138 539011	GB	MUW
SW.PA	Sodexo	15578 620750	FR	REX
SWED-A.ST	Swedbank AB	15047 719773	SE	BNK
SWMA.ST	Swedish Match AB	7821 532927	SE	TOB
SY1.DE	Symrise AG	12703 052600	DE	CHM
TATE.L	Tate & Lyle	4187 414119	GB	FOA
TEF.MC	Telefonica SA	32331 405964	ES	TLS
TEL.OL	Telenor ASA	23032 664468	NO	TLS
TEL2-B.ST	Tele2 AB B	8621 912671	SE	TLS
TELIA.ST	Telia Company AB	16151 169427	SE	TLS
TEMN.SW	Temenos Group AG	10213 002525	CH	SOF
TEN.MI	Tenaris SA	11864 396850	IT	OGX
TEP.PA	Teleperformance	12735 509400	FR	PRO
TIT.MI	Telecom Italia SpA	8459 017637	IT	TLS
TKA.DE	ThyssenKrupp AG	7495 285280	DE	IDD
TPK.L	Travis Perkins	4730 642257	GB	TCD
TRN.MI	Terna SpA	11913 412186	IT	ELC
TSCO.L	Tesco	29294 351743	GB	FDR
TUI1.DE	TUI AG	6612 159756	DE	TRT
UBI.PA	Ubisoft Entertainment SA	6939 327040	FR	IMS
UBSG.SW	UBS Group AG	43098 836809	CH	FBN
UCB.BR	UCB SA	13790 475400	BE	DRG
UCG.MI	Unicredit SpA Ord	28956 662280	IT	BNK
UG.PA	Peugeot SA	19272 836400	FR	AUT
UHR.SW	Swatch Group AG-B	7663 132882	CH	TEX
UMI.BR	Umicore	10683 904000	BE	CHM
UNA.AS	Unilever NV	79136 415440	NL	COS
UPM.HE	UPM-Kymmene Oyj	16448 725590	FI	FRP
URW.AS	Unibail Rodamco Westfield	19358 644050	FR	REA
UTDI.DE	United Internet AG Reg	6002 400000	DE	TLS
UU.L	United Utilities Group Plc	7602 365565	GB	MUW

Source: S&P Global and author.

Table A.28: *Firms Part X*

Ticker	Firm	Market Cap	ISO Code	Industry Code
VIE.PA	Veolia Environnement	13332 180420	FR	MUW
VIFN.SW	Vifor Pharma Group	10567 085500	CH	DRG
VIV.PA	Vivendi SA	30564 528280	FR	PUB
VNA.DE	Vonovia SE	26029 152000	DE	REA
VOD.L	Vodafone Group	49971 317452	GB	TLS
VOLV-B.ST	Volvo AB B	24537 431397	SE	AUT
VOW.DE	Volkswagen AG	51124 342500	DE	AUT
VWS.CO	Vestas Wind Systems AS	17918 957786	DK	IEQ
WDI.DE	Wirecard AG	13275 282500	DE	FBN
WEIR.L	Weir Group	4631 300556	GB	IEQ
WKL.AS	Wolters Kluwer NV	17751 500320	NL	PRO
WPP.L	WPP Plc	16725 083182	GB	PUB
WRT1V.HE	Wartsila Oyj ABP	5828 501100	FI	IEQ
WTB.L	Whitbread	8407 368452	GB	TRT
YAR.OL	Yara International ASA	10188 092051	NO	CHM
ZURN.SW	Zurich Insurance Group AG	55011 937615	CH	INS

Source: S&P Global and author.

Table A.29: *Countries*

ISO Code	Country	ISO Code	Country
AT	Austria	GB	United Kingdom
BE	Belgium	IE	Ireland
CH	Switzerland	IT	Italy
DE	Germany	LU	Luxembourg
DK	Denmark	NL	Netherlands
ES	Spain	NO	Norway
FI	Finland	PT	Portugal
FR	France	SE	Sweden

Source: S&P Global and author.

Table A.30: *Industries*

Industry Code	Industry
AIR	Airlines
ALU	Aluminum
ARO	Aerospace & Defense
ATX	Auto Components
AUT	Automobiles
BLD	Building Products
BNK	Banks
BTC	Biotechnology
BVG	Beverages
CHM	Chemicals
CMT	Communications Equipment
CNO	Casinos & Gaming
COM	Construction Materials
CON	Construction & Engineering
COS	Personal Products
CTR	Containers & Packaging
DHP	Household Durables
DRG	Pharmaceuticals
ELC	Electric Utilities
ELQ	Electrical Components & Equipment
FBN	Diversified Financial Services & Capital Markets
FDR	Food & Staples Retailing
FOA	Food Products
FRP	Paper & Forest Products
GAS	Gas Utilities
HEA	Health Care Providers & Services
HOM	Homebuilding
HOU	Household Products
ICS	Commercial Services & Supplies
IDD	Industrial Conglomerates
IEQ	Machinery & Electrical Equipment
IMS	Interactive Media, Services & Home Entertainment
INS	Insurance
ITC	Electronic Equipment, Instruments & Components
LIF	Life Sciences Tools & Services
MNX	Metals & Mining
MTC	Health Care Equipment & Supplies
MUW	Multi & Water Utilities
OGR	Oil & Gas Refining & Marketing
OGX	Oil & Gas Upstream & Integrated
PRO	Professional Services
PUB	Media, Movies & Entertainment
REA	Real Estate
REX	Restaurants & Leisure Facilities
RTS	Retailing
SEM	Semiconductors & Semiconductor Equipment
SOF	Software
STL	Steel
TCD	Trading Companies & Distributors
TEX	Textiles, Apparel & Luxury Goods
THQ	Computers & Peripherals & Office Electronics
TLS	Telecommunication Services
TOB	Tobacco
TRA	Transportation & Transportation Infrastructure
TRT	Hotels, Resorts & Cruise Lines
TSV	IT services

Source: S&P Global and author.

Bibliography

Acemoglu, Daron, Asuman Ozdaglar, and Alireza Tahbaz-Salehi (2015). "Systemic risk and stability in financial networks". In: *American Economic Review* 105.2, pp. 564–608.

Aielli, Gian Piero (2013). "Dynamic conditional correlation: on properties and estimation". In: *Journal of Business & Economic Statistics* 31.3, pp. 282–299.

Albert, Réka, Hawoong Jeong, and Albert-László Barabási (1999). "Diameter of the world-wide web". In: *nature* 401.6749, pp. 130–131.

Allen, Franklin and Ana Babus (2009). "Networks in finance". In: *The network challenge: strategy, profit, and risk in an interlinked world* 367.

Allen, Franklin and Douglas Gale (2000). "Financial contagion". In: *Journal of political economy* 108.1, pp. 1–33.

Anufriev, Mikhail and Valentyn Panchenko (2015). "Connecting the dots: Econometric methods for uncovering networks with an application to the Australian financial institutions". In: *Journal of Banking & Finance* 61, S241–S255.

Barigozzi, Matteo and Christian Brownlees (2019). "Nets: Network estimation for time series". In: *Journal of Applied Econometrics* 34.3, pp. 347–364.

Billio, Monica et al. (2012). "Econometric measures of connectedness and systemic risk in the finance and insurance sectors". In: *Journal of financial economics* 104.3, pp. 535–559.

Caccioli, Fabio, Paolo Barucca, and Teruyoshi Kobayashi (2018). "Network models of financial systemic risk: a review". In: *Journal of Computational Social Science* 1.1, pp. 81–114.

Carnero, M Angeles and M Hakan Eratalay (2014). "Estimating VAR-MGARCH models in multiple steps". In: *Studies in Nonlinear Dynamics & Econometrics* 18.3, pp. 339–365.

Demirer, Mert et al. (2018). "Estimating global bank network connectedness". In: *Journal of Applied Econometrics* 33.1, pp. 1–15.

Diebold, Francis X and Kamil Yilmaz (2009). "Measuring financial asset return and volatility spillovers, with application to global equity markets". In: *The Economic Journal* 119.534, pp. 158–171.

Diebold, Francis X and Kamil Yılmaz (2014). "On the network topology of variance decompositions: Measuring the connectedness of financial firms". In: *Journal of Econometrics* 182.1, pp. 119–134.

Diebold, Francis X and Kamil Yilmaz (2015). "Trans-Atlantic equity volatility connectedness: US and European financial institutions, 2004–2014". In: *Journal of Financial Econometrics* 14.1, pp. 81–127.

Elliott, Matthew, Benjamin Golub, and Matthew O Jackson (2014). "Financial networks and contagion". In: *American Economic Review* 104.10, pp. 3115–53.

Elliott, Matthew, Jonathon Hazell, and Co-Pierre Georg (2020). "Systemic risk-shifting in financial networks". In: *Available at SSRN 2658249*.

Epskamp, Sacha et al. (2018). "The Gaussian graphical model in cross-sectional and time-series data". In: *Multivariate behavioral research* 53.4, pp. 453–480.

Eratalay, M Hakan and Evgenii V Vladimirov (2020). "Mapping the stocks in MICEX: Who is central in the Moscow Stock Exchange?" In: *Economics of Transition and Institutional Change* 28.4, pp. 581–620.

Faloutsos, Michalis, Petros Faloutsos, and Christos Faloutsos (1999). "On power-law relationships of the internet topology". In: *ACM SIGCOMM computer communication review* 29.4, pp. 251–262.

Freixas, Xavier, Bruno M Parigi, and Jean-Charles Rochet (2000). "Systemic risk, interbank relations, and liquidity provision by the central bank". In: *Journal of money, credit and banking*, pp. 611–638.

Gai, Prasanna and Sujit Kapadia (2010). "Contagion in financial networks". In: *Proceedings of the Royal Society A: Mathematical, Physical and Engineering Sciences* 466.2120, pp. 2401–2423.

Horn, Roger A and Charles R Johnson (2012). *Matrix analysis*. Cambridge university press.

Iori, Giulia and Rosario N Mantegna (2018). "Empirical analyses of networks in finance". In: *Handbook of Computational Economics*. Vol. 4. Elsevier, pp. 637–685.

Jackson, Matthew O (2011). "An overview of social networks and economic applications". In: *Handbook of social economics*. Vol. 1. Elsevier, pp. 511–585.

Keeling, Matt J and Ken TD Eames (2005). "Networks and epidemic models". In: *Journal of the Royal Society Interface* 2.4, pp. 295–307.

Kenett, Dror Y et al. (2010). "Dominating clasp of the financial sector revealed by partial correlation analysis of the stock market". In: *PloS one* 5.12, e15032.

Killworth, Peter D and H Russell Bernard (1978). "The reversal small-world experiment". In: *Social networks* 1.2, pp. 159–192.

Krumsiek, Jan et al. (2011). "Gaussian graphical modeling reconstructs pathway reactions from high-throughput metabolomics data". In: *BMC systems biology* 5.1, pp. 1–16.

Kuzubaş, Tolga Umut, Inci Ömercikoğlu, and Burak Saltoğlu (2014). "Network centrality measures and systemic risk: An application to the Turkish financial crisis". In: *Physica A: Statistical Mechanics and its Applications* 405, pp. 203–215.

Lewis, Ted G (2011). *Network science: Theory and applications*. John Wiley & Sons.

Martinez-Jaramillo, Serafin et al. (2014). "An empirical study of the Mexican banking system's network and its implications for systemic risk". In: *Journal of Economic Dynamics and Control* 40, pp. 242–265.

Milgram, Stanley (1967). "The small world problem". In: *Psychology today* 2.1, pp. 60–67.

Millington, Tristan and Mahesan Niranjan (2020). "Partial correlation financial networks". In: *Applied Network Science* 5.1, pp. 1–19.

Opsahl, Tore, Filip Agneessens, and John Skvoretz (2010). "Node centrality in weighted networks: Generalizing degree and shortest paths". In: *Social networks* 32.3, pp. 245–251.

Pearson, Ronald K et al. (2015). "The class of generalized hampel filters". In: *2015 23rd European Signal Processing Conference (EUSIPCO)*. IEEE, pp. 2501–2505.

Plümper, Thomas and Eric Neumayer (2020). "Lockdown policies and the dynamics of the first wave of the Sars-CoV-2 pandemic in Europe". In: *Journal of European Public Policy* 0.0, pp. 1–21.

Solé, Ricard V et al. (2010). "Language networks: Their structure, function, and evolution". In: *Complexity* 15.6, pp. 20–26.

Watts, Duncan J and Steven H Strogatz (1998). "Collective dynamics of 'small-world'networks". In: *nature* 393.6684, pp. 440–442.

Willard, Stephen (2012). *General topology*. Courier Corporation.

Zachary, Wayne W (1977). "An information flow model for conflict and fission in small groups". In: *Journal of anthropological research* 33.4, pp. 452–473.

Symbol Index

$C_C^+(i)$	Positive closeness centrality of vertex i.
$C_D^{abs}(i)$	Absolute degree centrality of vertex i.
$C_D^{net}(i)$	Net degree centrality of vertex i.
$C_D^+(i)$	Positive degree centrality of vertex i.
$C_E^{abs}(i)$	Absolute eigenvector centrality of vertex i.
$C_E^+(i)$	Positive eigenvector centrality of vertex i.
$C_H^{abs}(i)$	Absolute harmonic centrality of vertex i.
$C_H^+(i)$	Positive harmonic centrality of vertex i.
$d(i,j)$	Distance from nodes i to j.
$\overline{d}(G)$	Average path length or average distance of graph G.
$\mathrm{diam}(G)$	Diameter of graph G.
$h(G)$	Homophily ratio of graph G.
$h^*(G)$	Homophily baseline ratio of graph G.
$m(G)$	Number of edges of the network G.
N	Number of vertices of the network.
$\mathrm{rad}(G)$	Radius of graph G.
$w(ij)$	Weight of the edge ij.
$w(G)$	Weight of the graph G.

Acknowledgements

I wish to express my deepest gratitude to Hakan Eratalay, my supervisor, who lead me throughout the way with tons of patience. I would like to especially thank Jaan Masso for his support during the master's program. And to my family, I want to thank them with all my heart for their support and encourage me to undertake this adventure, especially Jesús Alva, my husband, who has been with me all the way and who also helped me review my work and gave me advice. As always, any errors or oversights are mine alone.

Lühikokkuvõte

Käesoleva uurimuse eesmärk on analüüsida võrgustiku topoloogiat Euroopa aktsiaturu, eelkõige S&P Euroopa indeksisse kuuluvate aktsiate vastastikuste seoste põhjal, kasutades andmeid perioodist 2016. aasta jaanuar kuni 2020. aasta september.

Arvutasime välja indeksi päevased tootlused logaritmitud hindade muutustena, ja kasutasime tinglike korrelatsioonide saamiseks mõjusat dünaamilise tingliku korrelatsiooni mudelit; niiviisi saime osalise korrelatsioonivõrgustiku, kasutades Gaussi graafilise mudeli algoritmi. Osalise korrelatsioonivõrgustiku koostamiseks kasutasime seejuures külgnevusmaatriksina osakorrelatsiooni kordajate maatriksit. Seetõttu on meil korrelatsioonikordajatel nii negatiivsed ja positiivsed väärtused; sel põhjusel võtsime analüüsis arvesse nii netoandmeid (algväärtusi), absoluutandmeid (algväärtuste absoluutväärtust) kui ka positiivseid andmeid (ainult positiivsed väärtusi).

Me teostasime võrgustiku analüüsi COVID-19 pandeemiaga külgnevatel ajaperioodidel, kus lisaks kogu ajavahemikule võtsime analüüsis arvesse nelja perioodi: jaanuar 2016-oktoober 2019 (COVID-19 pandeemiale eelnev periood), november 2019 – veebruar 2019 (COVID-19 pandeemiale vahetult eelnev periood), märts-juuni 2020 (COVID19 pandeemia esimesed kuud) ja juuli-septemer 2020.

Analüüsis arvutasime välja võrgustikus servade arvu ja kogukaalu. Lisaks arvutasime välja võrgustiku keskmise kauguse, võrgustiku läbimõõdu ja esimest korda finantsvõrgustike alases uurimistöös ka võrgustiku raadiuse, mis täiendab muid globaalseid võrgustike mõõdikuid. Need kolm viimast parameetrit võimaldavad meil tuletada jõu, mida majanduslik ebastabiilsus peaks aval-

dama võrgustikus kaskaadefekti käivitamiseks.

Lokaalsete mõõtude põhjal arvutasime välja astme, läheduse, harmoonilisuse, vahepealsuse ja omavektori tsentraalsused, et mõõta ettevõtete olulisust võrgustikus eri aspektidest, nagu seoste tugevus oma ümbruskonnaga ja nende asukoht võrgustikus. Võrgustiku tsentraalsuse mõõdikute teadmine võimaldab keskpankadel määrata globaalse süsteemselt olulise ettevõtja asukoha ja seega neid reguleerida.

Dünaamilise võrgustiku kontseptsiooni raamistiku rakendamisega tuvastasime komponentide vaheliste seoste stabiilsuse ja COVID-19 pandeemia ajal tuvastasime seoste stabiilsuse olulist tõusu.

Teostasime esmakordselt finantsvõrgustike analüüsi kontekstis homofiilse profiili analüüsi ning analüüsides ettevõtteid riikide ja sektorite kaupa leidsime ettevõtete vahel vägagi homofiilsed suhted. Põhjalikumaks analüüsimiseks võtsime arvesse osakorrelatsioonide erinevaid katkepunkte ja märkasime otsest seost osakorrelatsioonide ja homofiilsuse proportsiooni vahel võrgustikus, millel puhul tuvastasime kõrgemate korrelatsioonikordaja väärtuste korral suurema homofiilsuse. Homofiilsus on sotsiaalvõrgustike analüüsi kontektsis väga populaarne mõiste, samas rahanduses on seda autori teadmiste kohaselt ainult mainitud ilma põhjalikumalt kasutamata.

Varasemates uuringutes on empiirilised tulemused näidanud, et pärast kriisi võrgustiku seotus suureneb; seevastu antud analüüsis käsitletud võrgustiku puhul, kasutades viitena COVID-19 šokki ja dünaamilise võrgustiku raamistikku, tuvastasime pandeemia ajal hoopiski suhete stabiilsuse kasvu. Siiski ei saa eelnevast tingimata järeldada, et võrgustiku osaliste seas oleks seotus suurenenud.

Non-exclusive licence to reproduce thesis and make thesis public

I, Ariana Paola Cortés Ángel (7th March 1986),
herewith grant the University of Tartu a free permit (non-exclusive licence) to:

1. reproduce, for the purpose of preservation, including for adding to the DSpace digital archives until the expiry of the term of copyright,

   Deep Diving into the S&P 350 Europe Index Network and Its Reaction to the COVID-19

   supervised by

   M. Hakan Eratalay,

2. I grant the University of Tartu a permit to make the work specified in p. 1 available to the public via the web environment of the University of Tartu, including via the DSpace digital archives, under the Creative Commons licence CC BY NC ND 3.0, which allows, by giving appropriate credit to the author, to reproduce, distribute the work and communicate it to the public, and prohibits the creation of derivative works and any commercial use of the work until the expiry of the term of copyright.

3. I am aware of the fact that the author retains the rights specified in p. 1 and 2.

4. I certify that granting the non-exclusive licence does not infringe other persons' intellectual property rights or rights arising from the personal data protection legislation.

Ariana Paola Cortés Ángel

Tartu, 24.May.2021